Final Report
NASA, Langley Research Center
NSG-1138

THE EFFECTS OF THE LAMINAR/TURBULENT BOUNDARY LAYER STATES ON THE DEVELOPMENT OF A PLANE MIXING LAYER

Prepared by
J.F. Foss

Department of Mechanical Engineering and
Division of Engineering Research
February 27, 1977

Final Report
NASA, Langley Research Center
NSG-1138

The Effects of the Laminar/ Turbulent Boundary Layer States on the Development of a Plane Mixing Layer

Prepared by
J.F. Foss

Department of Mechanical Engineering and
Division of Engineering Research
February 27, 1977

An investigation of the initial conditions effects on the plane mixing layer has been executed; a report of this study is presented herein. The investigation was initiated in 1972 and was motivated by the apparent conflict between (i) the accepted tenent of self-preserving flows that ..."the conditions at the initiation of the flow are largely irrelevant," ... Townsend [1975]*, and (ii) the comparison of the Liepmann and Laufer [1947] and Wygnanski and Fiedler [1970] results which suggested that the initial conditions influence persists in the self-preserving or asymptotic state. More specifically, the comparison suggests that the initially turbulent layer is relatively wider (i.e., spreads more rapidly) than the initially laminar layer.

An extended discussion of the extant literature and the present experimental techniques, results and conclusions has been prepared as a manuscript for the Symposium on Turbulent Shear Flows.** Since this document contains the technical material which represents the technical report of the research work (partially) supported by the NASA Grant NSG-1138, it was decided to include the Symposium manuscript as an Appendix to this report and to have it serve as the communication of the technical results. This decision has been essentially, but not strictly, carried out. The first complete draft of the Symposium manuscript exceeded the maximum length limitation; hence, the text of the Symposium manuscript was necessarily reduced and several of the figures were reduced in size. These reductions were not necessary for the present communication; the unabridged version of the manuscript is presented as Appendix A. The original boundary layer and shear layer data are reproduced as Appendix B.

*This and other cited references may be found in Appendix A.

**The Pennsylvania State University, University Park, PA, 18-20 April 1977.

Appendix A

Original version of the abridged manuscript submitted for the Symposium on Turbulent Shear Flows", the Pennsylvania State University, University Park, Pennsylvania, April 18-20, 1977.

THE EFFECTS OF THE LAMINAR/TURBULENT BOUNDARY LAYER STATES ON THE DEVELOPMENT OF A PLANE MIXING LAYER

John F. Foss
Department Mechanical Engineering
Michigan State University

ABSTRACT

The effect, of the laminar/turbulent boundary layer state on the mean and rms velocities of a developing plane mixing layer, has been investigated. The maximum Ux/ν allowed by the facility was 6.7 x 10^5; the maximum x station surveyed corresponds to approximately 1800 and 630 initial momentum thicknesses for the laminar and turbulent cases respectively. The use of commonly accepted non-dimensional representations of the data confirm (at least) an approximately self-preserving condition. They also suggest that the effects of the laminar/turbulent initial condition persist in the self-preserving region. A direct comparison of the data reveals that the persistence so observed is illusory. An interpretation of the reason for this misunderstanding is advanced.

NOMENCLATURE

Symbol	Definition
B	parameter used in transformation of laboratory to standard Gaussian coordinates, see (ζ)
E	Hot-wire voltage
E_o,K,n	coefficients in the hot-wire response equation (1)
H	δ_d/θ, boundary layer shape parameter
LBL	the case for which the boundary layer at x = 0 is laminar
m	parameter used in transformation of laboratory to standard Gaussian coordinates, see Table 2 for m_i where i=1,....4
p	static pressure
q	mean velocity vector in the undisturbed (streaming) fluid
Re_θ Re_x	Reynolds numbers based upon θ and x
S.P., St	designation of mixing layer from splitter plate (S.P.) and backward facing step (St)
S.D.	standard deviation defined for Gaussian fit to $\bar{u}/U$ data, see Table 2 for SD_i, i=1..4
TBL	the case for which the boundary layer at x = 0 is turbulent
u, v, w	velocity components in the mixing layer
u_τ	wall shear stress velocity $(\tau_w/\rho)^{1/2}$
U	i) component of q ii) reference velocity for mixing layer St $\lim_{y\to\infty} u(x,y)\to U$; S.P. $\lim_{y\to\pm\infty} u(x,y)\to U_1, U_2$
V	i) component of q ii) magnitude of the velocity vector in the xyplane $V^2=(u^2+v^2)$
x,y,z	longitudinal, lateral, and span wise position coordinates
x_o	apparent origin (defined for the specified width measure) of the mixing layer
y(r)	y location at which u/U = r
δ,δ_d,θ	boundary layer, displacement, and momentum thicknesses
δ_ω	vorticity thickness ≡ $(U_1-U_2)/\{(\partial\bar{u}/\partial y)$ at $y(0.5)\}$
σ_f	Görtler constant: $u/U = \mathrm{erf}\{\sigma_f(y-y(0.5))/(x-x_o)\}$
σ_p	standard deviation of Gaussian distribution
ζ ≡	my + B, ζ is argument of standard Gaussian: mean = 0, σ_p = 1

Super and sub scripts

$(\bar{})$ $(\tilde{})$	temporal average and r.m.s. of ( )
$(\ )_i$	initial condition of ( ); ( ) at x = 0

INTRODUCTION

Plane mixing layers. The plane mixing layer is a comparatively simple, yet technologically important turbulent flow field. The literature on it is correspondingly vast. Because of its simplicity - absence of direct influence of a solid surface, shear stress of one sign, linear growth rate in its asymptotic region - and because the classical process of energy production, dissipation, etc., are present in addition to the self-preservation and entrainment phenomena, the plane shear layer has served as a subject flow for the study of basic turbulence processes.

The recent identification of large scale, coherent motions (1), (2) in the layer, and the recognition that these are possibly the controlling agents for its growth, has induced even more interest in this flow. The technological importance of the plane mixing layer for aerodynamic and chemically reacting flows is made apparent in the reports of specialist's conferences on the respective subjects (3), (4). The latter contains an extensive review and interpretation of the available literature (on plane mixing layers) by Murthy (4).

The phenomena of self-preservation is of particular interest for the present study; the defining remarks by Townsend (5, p. 169) are useful for the clarification of its meaning and for later reference.

> "The principle, as distinct from the assumption, of self-preservation asserts that a moving equilibrium is set up in which the conditions at the initiation of the flow are largely irrelevant, and so the flow depends on one or two simple

parameters and is geometrically similar at all sections."

Two general classes of plane mixing (or free shear) layers can be identified. Birch and Eggers (3) refer to these as: (i) layers which are created from a splitter plate (S.P.) with unsheared velocities U_1 and U_2, and (ii) layers which form downstream of a backward facing step (St.) and involve a single stream which enters a "quiescent" ambient fluid. For (i), a "simple parameter" would be a representation of the velocity ratio such as $(U_1 - U_2)/(U_1 + U_2)$. Superficially, case St may be described as the limiting condition of case S.P. where $U_2 \to 0$. However, the entrainment process can be expected to be quite different, if $\vec{q}_2 = \hat{i}\, U_2$, (case S.P.) vs $\vec{q}_2 = \hat{j}\, V_2$ (case St.), and, in particular, dramatic differences can be expected near the origin.

An interesting feature of the plane mixing layer is the absence of an intrinsic length scale for the "idealized" case. The lateral dimension of the splitter plate trailing edge provides a reference length which must be of some importance quite close to the plate but it is possible to make this dimension hydrodynamically small; see Chevray and Kovasznay (14). An extrinsic length scale is present in all (real) plane mixing layer flows; the boundary layer(s) length parameters, at the initiation of the layer, represent these extrinsic length scales. The plausible expectation that the boundary layer momentum thickness is the appropriate reference length to characterize the developing region was first systematically studied by Bradshaw (6) in an investigation of the axisymmetric mixing layer downstream of a 5 cm diameter jet orifice. Bradshaw identified quantitative requirements for the development length which is necessary to achieve a self-preserving flow; he has also cautioned* against the misuse of these criteria. From the defining remarks regarding self-preservation and from the recognition that δ_i, δ_{di} and θ_i are the available length scales to characterize the plane mixing layer, one could expect that the sole effect of the initial ($x = 0$) conditions would be to alter the development length to achieve self-preservation.

Wygnanski and Fiedler (7) undertook a comprehensive investigation of a plane mixing layer in order to extend the data base, by including conditionally sampled measurements, beyond that provided by the earlier and widely accepted results of Liepmann and Laufer (8). Surprisingly, and strikingly given the above considerations, the two studies showed pronounced differences in even the simplest measure of the flow . . . the spreading rate of the mean velocity distributions in the "asymptotic" region. The inference was made that the asymptotic region was influenced by the conditions at the origin of the shear layer!

This possibility, and the desire to evaluate it by comparative measurements in the same (!) flow system provided the motivation for both the present investigation and that of Batt (9). Batt used a flow system which allowed the shear layer growth in the tripped and untripped S.P. and St configurations to be evaluated. The trip wire in Batt's experiment provided a "disturbed" ($\tilde{u}/U_1$ max. $\approx 12\%$) laminar ($\tilde{u}/U_1$ vs y/δ_d is "identical" with that of the Blasius solution) boundary layer at $x = 0$. His results confirm that a residual effect of the boundary layer state is present in the (apparently) asymptotic region as defined by the longitudinal independence of the normalized $\bar{u}$ and u distributions. (This is the accepted criterion for self-preservation in plane shear layers (5).) A similarly motivated investigation has quite recently been executed by Browand (10) in a two stream mixing layer ($U_2/U_1 = 0.23$). The effect of the initial condition was seen to persist over the range of his measurements. For $0 \le x/\theta_i \lesssim 500$, the growth rate of the LBL condition was larger than that for a turbulent boundary layer at $x = 0$. For $x/\theta_i \gtrsim 500$ the growth rate of the T.B.L. condition was observed to approach that of the LBL condition. A comparison of the Batt (9) and Browand (10) results suggests that the St and S.P. flows may be fundamentally different. This comparison would also support the contention that more data at quite large Re_x values are required to resolve the question of the initial conditions influence on the asymptotic state.

The spreading rate, as defined by the mean velocity field, and the maximum fluctuation intensity are representative of the measures used to describe the time mean flow field. The engineering interest in these measures of the complex, time dependent flow field is both well established and well motivated for the purposes of analysis and design. However, the (net) cause for these observed effects is best sought in terms of the governing phenomena which are responsible for the behavior of the shear layer. Specifically, the influence of the initial conditions on the growth and interaction of the large scale coherent motions is recognized as the central question given the current understanding of the controlling phenomena within a shear layer. Champagne, et. al. (11) offer some interpretive remarks in this regard in addition to their original results regarding the behavior of the shear layer. The qualitatively reasonable suggestion that the initial turbulence structure inhibits the vortex pairing processes is advanced. Since this "disruption" of the otherwise orderly processes is likely to be particular to a given flow, they further suggest that the self-preserving condition may also be particular and not universal. A second interpretive observation (originally suggested by Laufer and Browand) is that contamination from the side wall boundary conditions may dominate many large Re_x flows. The suggestion is made that if the spacing between adjacent vortical elements, normalized by the flow width, exceeds $\simeq 0.25$, then a transverse flow in the core of the element can be expected. An increase in the turbulence fluctuation level and the entrainment rate are caused by this contamination. The authors (11) observe that the good agreement between their results and those of Patel (13) are encouraging in the search for the universal, asymptotic, shear layer; they site this agreement as an indication that the possible contamination has not influenced either set of results. The lack of documentation for the initial boundary layer state in either of the latter two flows will make it difficult to use their results in the interpretation of the initial conditions effects.

Dimotakis and Brown (12) offer an extensive, and well-considered, discussion of the initial-conditions influence on the flow field as interpreted through the behavior of the large scale structures. They present a persuasive argument that the approach to the asymptotic state may be extremely slow and that the apparent asymptotic states observed in laboratory flows are merely in the (slowly varying) intermediate stage of their development. They cite, as a reason for this, that the growth rate (e.g., $d\delta_\omega/dx$) is possibly a function of the vorticity distribution within the shear layer and since this distribution can be expected

*See the discussion on p. 39 of (3). Bradshaw notes that the required distance for the developing region, in terms of θ_i units and the R_x requirements may be sensitive to $(U\theta_i/\nu)$.

to change slowly, the approach to the final growth rate is correspondingly gradual.

THE PRESENT INVESTIGATION

The objectives of the present study may be readily formulated given the above considerations. Its principle objective is to provide sufficient measurements, of the spatial distributions for the first and second moments of the velocity in the developing region of a plane shear layer, that the influence of the laminar/turbulent initial boundary layer states can be assessed. The need for this study is implicit from an assessment of the previous investigations: there has been no direct comparison of the shear layers which result from the laminar/turbulent initial boundary layer conditions (in the same apparatus) for the St configuration. (It can be added that measurements beyond the region of rapid development were desired but that the above noted cautions regarding a "universal asymptotic state" are responsible for the stated interest in the developing region. Secondary purposes are: (i) to provide a data base with appropriate documentation that can serve as a test case for calculation methods* and (ii) to provide the basis for further studies which will seek to establish the governing phenomena which are responsible for the (presently) observed behavior of the time mean flow field.

EXPERIMENTAL FACILITY

A schematic representation of the experimental facility which is capable of providing a laminar or turbulent boundary layer at the initiation of the shear layer is shown in Figure 1. A large centrifugal fan (outlet dia = 40cm) is used to pressurize the 100 x 150cm plenum chamber which supplies air to the symmetrical contraction. The final flow control elements (straw-honeycomb and 30 mesh screen) result in a free stream fluctuation intensity of 0.2% at x = 0 for a flow velocity of 18.3mps. The fluctuations in the y and z directions are undoubtedly greater; they were not measured. The rectangular opening is 9.4 x 100cm and the vertical walls at x = 0 and z = ±50cm are shown to scale. A traverse rig (not shown) was supported on roller bearings at z = ±60cm and rode above the lateral walls. An LVDT sensor monitored the position of the probe over the range ±76mm with a resolution of ±.03mm.

The laminar/turbulent boundary layer state was controlled by the suction/blowing ondition of the discrete, rectangular (11 x 25mm) openings above the gap created by the end of the contraction and the leading edge of the smooth boundary layer plate. The details of this configuration are shown in Figure 2. The 1.8mm vertical displacement and the 10mm gap length were selected after a trial-and-error search for the minimum disturbances (at x = 0) for the laminar boundary layer (L.B.L.). A negative pressure of $[0.95\rho U_1^2/2]$, similarly determined, was maintained in the super plenum for the L.B.L. condition. A positive pressure of $[0.1\rho U_1^2/2]$ was required to gain a fully turbulent boundary layer for all z locations. An interesting feature of the flow system is the intermittent laminar/turbulent boundary layer state for no suction or blowing; this condition would allow the interesting study of the downstream propagation/contamination of the initial condition to be examined via conditional sampling techniques. It is noteworthy that the discrete sections and tubing connections were both necessary and sufficient to gain a spanwise independent suction/blowing system. The initial attempt at boundary layer control with a similar configuration,* viz., a simple gap opening into a plenum, produced both a Helmholtz resonant frequency (not observed in the present data) and a laminar boundary layer only over a short central span of the shear layer. The results of these boundary layer control efforts are presented in the Results section.

*The results of the measurements are available on IBM cards in a Fortran compatible format. They are available, at cost, upon request.

DATA ACQUISITION AND SIGNAL PROCESSING

The time mean and r.m.s. values of the velocity, which are presented in the Results section, have been obtained using a single hot-wire probe set parallel to the z-direction. The probe configuration (Disa 55 F 11) is somewhat sensitive to pitch effects; however, the maximum error is approximately 5% (at 90 degrees), see Comte-Bellot, et. al, (15) which is considered to be satisfactory considering the objectives of the present study.

The calibration of the hot-wire was accomplished in the free stream of the flow from the main plenum. The total pressure was measured with a capacitive pressure transducer (Decker 308-3); the transducer linearity specifications and the $V\text{-}p^{\frac{1}{2}}$ relationship combine to yield an accuracy of ≈±0.18mps for 3≤V≤37mps. The bridge voltage of the hot-wire anemometer (T.S.I. 1054-A) was conditioned (T.S.I. 1057) by a 10Khz low pass filter and a 2 volt suppression in order to respectively eliminate a substantial portion of the (high frequency) anemometer noise and to reduce the dynamic range (0-2 vs 0-4 volts) for the subsequent A/D conversion. The residual and amplified anemometer noise is nominally 3mv; as such it will, at most, effect the 1.s.b. of the 5mv resolution A/D converter. An on-line T.I. 960A minicomputer was used to create and store an ensemble average of the samples collected over the specified time period. The calibration data were formed from 10^4 simultaneous samples of the hot-wire and pressure transducer voltages at a given flow speed. These values were averaged and 12-15 such data pairs were used to evaluate the constants E_o^2, K and n in the expression

$$E^2 = E_o^2 + KV^n \qquad (1)$$

A constant value of the exponent n is supported by the results of Brunn (16) for the range 3≤V≤20mps of interest in this work. The standard deviation of the calibration data was typically 0.06mps. (It is assumed for this calculation that the hot-wire voltage measurement and equation 1 are precisely correct.)

The L.B.L. flow field data were processed with the same routine; the hot-wire voltage was sampled and averaged for 10 seconds at each location of the traverse. In addition, an r.m.s. voltmeter (Disa 55 D 35) was used to convert the voltage vluctuations into an analog voltage which was proportional to ē of the original signal. This analog voltage was recorded, along with the LVDT output signal, and the three average values were stored for further processing. The 10 second averaging time appeared to give satisfactory results and it was anticipated that a large number of (statistically independent) samples across

*The same 15 h.p. suction blower was used in the initial attempt.

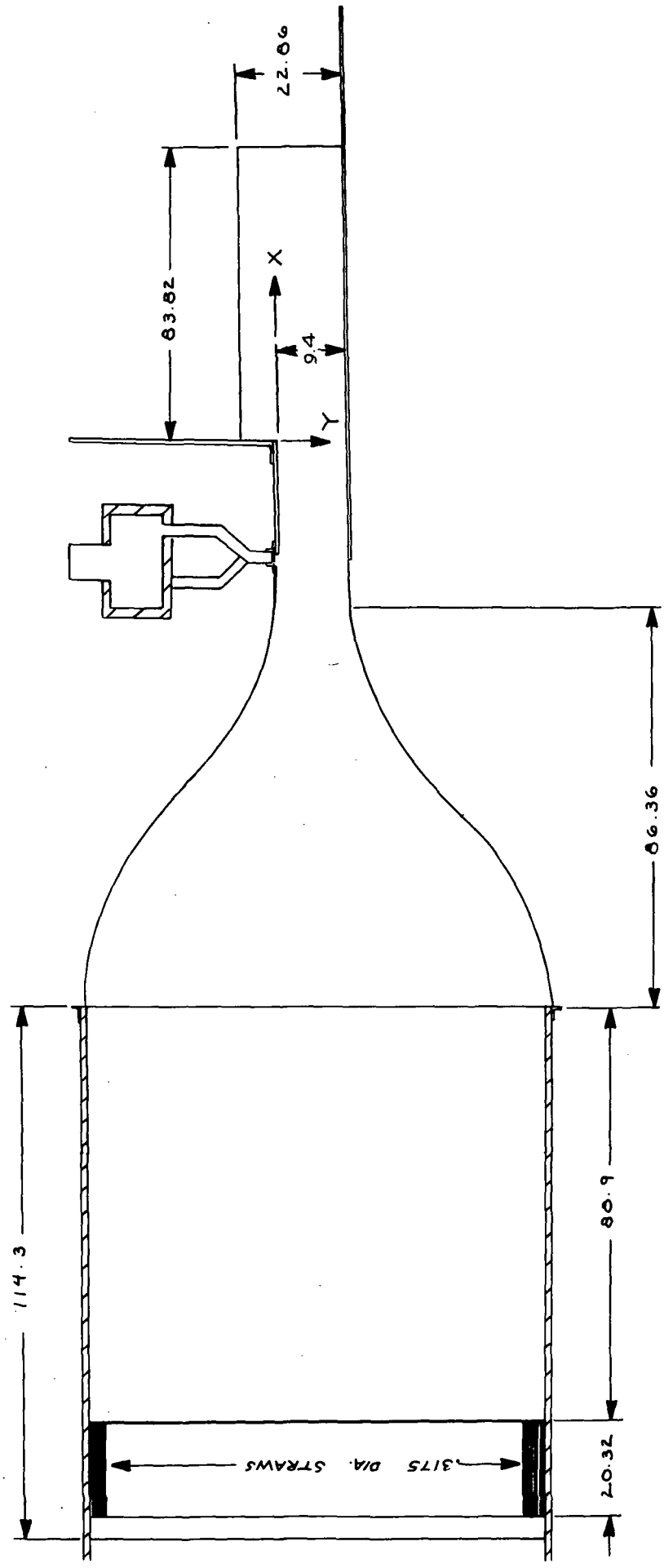

Fig. 1. Schematic representation of flow system

Note: Fan, wide angle diffuser, turning vanes and rubberized horsehair flow straightener =2.1m upstream of soda straw honeycomb) are not shown. dimensions in cm.

the physical traverse would provide acceptable data. This was subsequently confirmed as regards the general trends of the velocity field behavior; however, detailed consideration of the growth characteristics of the layer were later inferred to require both longer sampling times and more spatial locations. The acquisition software was altered to allow an arbitrary sampling period and the TBL results were collected for 60 second time periods.

The r.m.s. velocity fluctuation $\tilde{u}$ was calculated from the measured $\tilde{e}$ by the relationship:

$$\tilde{u} = \tilde{e}\langle(dV/dE)\rangle \qquad (2)$$

where $\langle(dV/dE)\rangle$ is evaluated from (1) at the ensemble average $\langle E\rangle$ value. The maximum error resulting from the constant slope assumption in this calculation is estimated by comparing $\tilde{u}$ with the average magnitude of $[V(E \pm \tilde{e}) - V(E)]$ for the largest $\tilde{e}\langle(dV/dE)\rangle$ values of the final data set. A representative value for the error is 0.8% for the x = 508mm traverse with the turbulent boundary layer initial condition. The fluctuating velocity is, of course, influenced by the transverse (v) component and the second order effects of u. A consideration of these higher order effects readily shows that the interpretation of the mean and r.m.s. voltages is both ambiguous and quite complex. No higher order corrections were made.

RESULTS

Boundary Layer Survey

Velocity traverses at selected span wise locations were used to document the boundary layer at x = -2mm. These data are to characterize the initial condition for the shear layer. A zero y position was inferred from the $\bar{u}(y)$ data and an integration routine was used to evaluate δ_d and θ for each traverse. The composite results are presented in Table 1.

A very substantial effort was required to completely eliminate the presence of turbulent bursts for the LBL condition. The problem was localized near z=42 and 58cm; interestingly, z=50cm was a region of very little disturbance. The problem was traced to slight

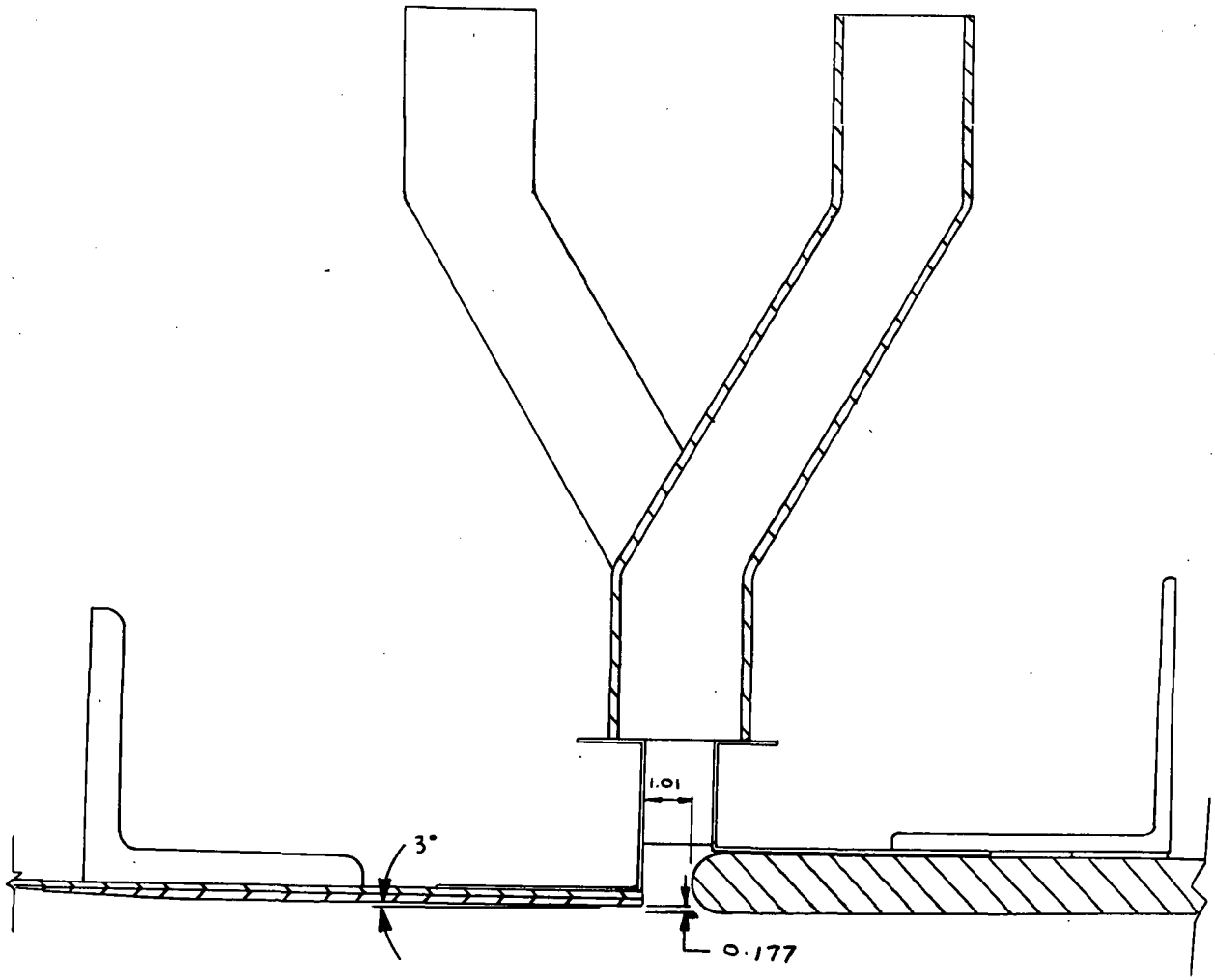

Fig. 2. Detail of the Suction and Blowing Scheme for the LBL and TBL Conditions

irregularities in the surface and was controlled in that a completely laminar state existed for the LBL case. However, the laminar boundary layer at z=42cm was strongly disturbed with an r.m.s. fluctuation level higher than that of the turbulent boundary layer. The fluctuations of the LBL case were quite different from the (spectrally rich) fluctuations of the TBL case; oscillograph traces of the two cases are presented in Figure 3.

Table 1. Summary of Boundary Layer Data

	z	U(mps)	δ(mm)	θ(mm)x10^1	δ_d/θ	R_θx10^3	$\tilde{u}_{max}/U$
LBL:	20	18.3	1.9	2.6	1.9	0.34	4.1
	42	18.3	2.4	3.0	1.9	0.39	11.4
	50	18.2	1.9	2.7	2.2	0.36	3.4
	58	18.3	2.2	3.1	2.3	0.40	6.8
	71	18.3	2.1	2.8	2.4	0.37	3.3
	86	18.3	2.2	2.9	2.3	0.37	6.1
TBL:	42	18.4	10.0	10	1.3	1.4	9.7
	50	18.4	6.5	6.6	1.5	0.9	9.7
	58	18.4	8.6	9.0	1.4	1.2	8.9
	71	18.4	7.5	8.1	1.5	1.1	9.8

The shear layer data were taken at the location of the minimum disturbance condition, z=71cm. The specific boundary layer conditions at this z location are presented in Figures 4 and 5. Close agreement between the present and the "standard" turbulent boundary layer, Coles (17), is evident. (u_τ was evaluated from the three "wall-law" points as plotted on a Clauser plot (18). u_τ=0.85mps.) The LBL/Blasius solution comparison suggests that the suction scheme results in a distorted profile $[u_\tau\delta_d/\nu]$(present) > $[u_\tau\delta_d/\nu]$(Blasius). Figure 6 presents the ũ/U data for the LBL and TBL cases.

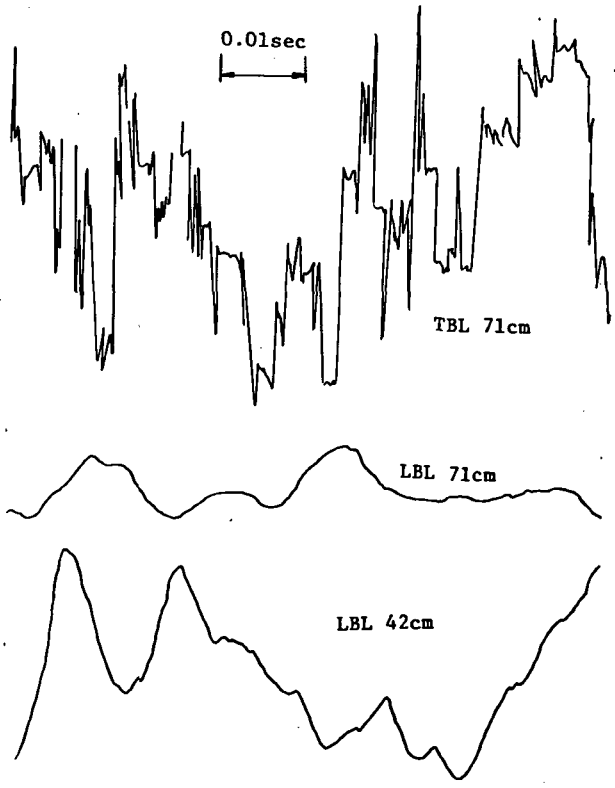

Fig. 3. Oscillograph traces of E(t) at u/U=0.5, x=0. (Amplitude is arbitrary and constant for all traces.)

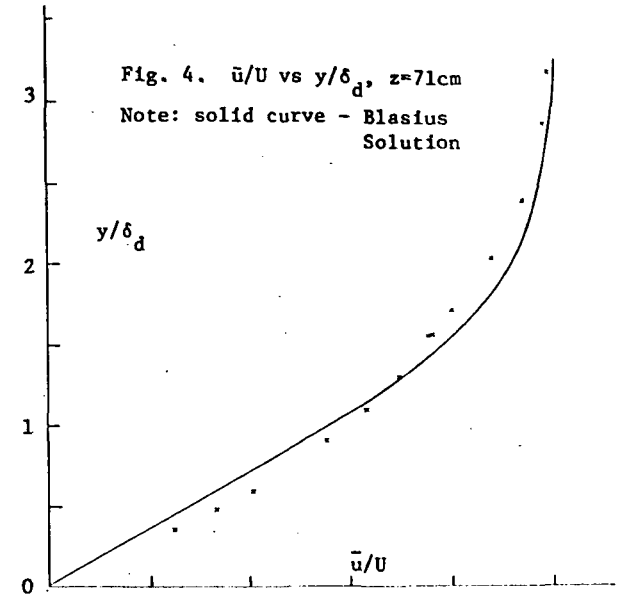

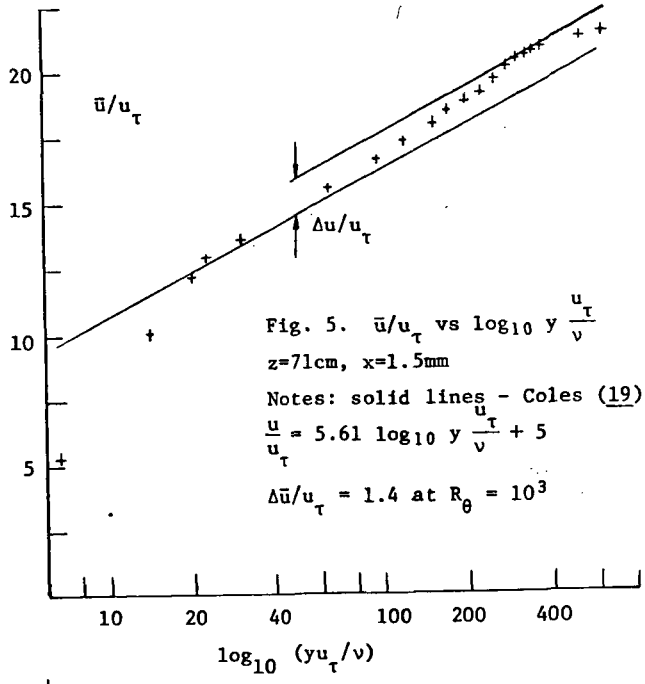

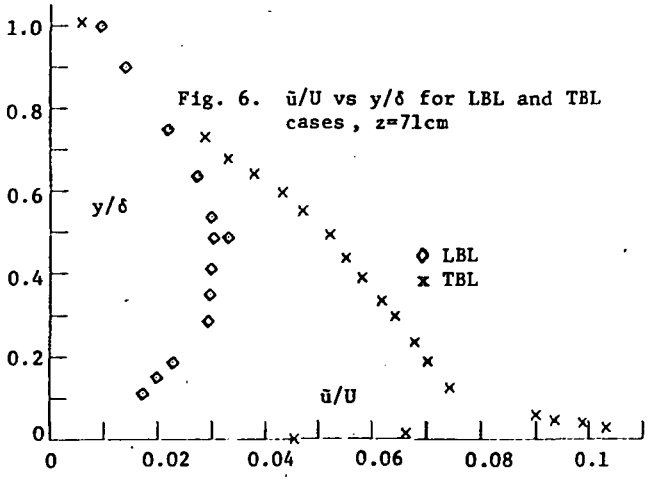

Shear Layer Survey

The composite mean and r.m.s. values of the velocity are presented in Figures 7 and 8. The normalization of the y dimension, viz. [y-y(.5)]/x, is used to provide a compact presentation; the self-similar character of these data is considered in the next section. The maximum x location surveyed was x=50.8cm; this location is the farthest downstream location for which the infrequent turbulent signals, occurring at y=5cm, could be reliably traced to either the shear layer or the lower plate boundary layer. Hence, beyond this location, the shear fields of the two streams interact. The two streams interact much farther upstream in terms of the pressure fluctuations induced by their irregular boundaries. These fluctuations are observable as very low frequency, but substantial amplitude u fluctuations in the region of the flow between the two developing layers.

DISCUSSION OF RESULTS

Evaluation of Shear Layer Width

The evaluation of the plane mixing layer growth rate is facilitated by the definition of an appropriate width measure of the mean velocity field. If the flow is self-preserving, then all measures are in fixed proportion and the selection of a particular width measure may be arbitrarily made. If the developing shear layer is to be characterized, then judgement in the selection must be exercised. A desirable characteristic of the width measure is that it not rely upon the measurement of a specific velocity value; rather, it is preferable that it represent a smoothed measure of several independent velocity measurements. The momentum thickness (θ) utilized by Winant and Browand (2) is compatible with these criteria. However, it is inappropriate to calculate θ using single-wire measurements for the St case since $|V|$ does not approach zero as $y \to -\infty$ and (consequently) the integral of the experimental data is not well defined.

The use of an approximate analytic form which involves a width measure as a parameter is an appropriate response to the stated criteria; the use of the error function (erf) as the analytic form is adopted for this purpose. As will be quite evident, it is not assumed that the erf can be used to describe $\bar{u}$ for all y; indeed, this fitting process will allow the agreement between the data and this analytic expression to be evaluated. The fit, over the region of interest, is accomplished by using the measured $\bar{u}/U$ to evaluate ζ as:

$$\frac{\bar{u}}{U} = 0.5 + \text{erf}\,\frac{\zeta}{\sqrt{2}} \tag{3}$$

where ζ is the argument of the Standard Gaussian cumulative distribution function

$$F(\zeta) = \frac{1}{\sqrt{2\pi}} \int_{-\infty}^{\zeta} \exp\left[\frac{-\alpha^2}{2}\right] d\alpha \tag{4}$$

(Note that F has its mean value at ζ=0 and the standard deviation of the distribution is obtained at ζ=1.) Since the experimental data exists in pairs as (u/U,y), it is possible to form the relationship

$$\zeta = my + B \tag{5}$$

Consequently, m and B can be found from an application of a least squares relationship to the (ζ,y) pairs. Using (3) and (5), the centerline of the mean velocity traverse is seen to be

$$y(0.5) = -B/m \tag{6}$$

and the quantity m^{-1} is seen to be the standard deviation of the spatial distribution, viz.,

$$\pm\, m^{-1} = y(0.5 \pm 0.341 \ldots) - y(0.5) \tag{7}$$

The quality of the fit can be assessed by evaluating the standard deviation (S.D.) between the measured $\bar{u}/U$ and that computed from (3). This procedure has been carried out for four cases; the corresponding m and S.D. values are identified by the subscript numbers $1 \to 4$ which refer to a subset of the $\bar{u}/U$ values as described in Table 2.

The Görtler (19) solution can be written as

$$\frac{\bar{u}}{U} = 0.5 + \text{erf}\ \sigma_f\{\frac{y-y(.5)}{x-x_o}\} \tag{8}$$

which is related to m_1 by the expression

$$\sigma_f = \frac{m_1(x-x_o)}{\sqrt{2}} \tag{9}$$

The vorticity width δ_ω, which is defined as

$$\delta_\omega \equiv U/(\frac{\partial u}{\partial y})_{y(0.5)}$$

can be evaluated as

$$= \{\frac{\partial(u/U)}{\partial\zeta}\Big|_{\zeta=0}(\frac{\partial\zeta}{\partial y})\}^{-1} = \sqrt{2\pi}/m_2 \tag{10}$$

The full set of m^{-1} values are presented in Figure 9; the standard deviations are presented in Table 3. These results can be summarized as follows:

1) The Görtler solution and the high velocity side of the mixing layer are not well fit by the error function (SD≅3%) whereas the central region and the low velocity side of the shear layer are quite closely approximated by this analytic form (SD<1% ... for sufficiently large x).

2) The m_2^{-1} distributions suggest the x_o values:

$$x_o(\text{TBL}) = +7.5\text{cm},\ x_o(\text{LBL}) = -4.1\text{cm} \tag{11}$$

3) The spread constants, evaluated from m_1^{-1} are:

$$\sigma_f(\text{TBL}) = 10.19,\ \sigma_f(\text{LBL}) = 13.6 \tag{12}$$

which are somewhat different from the disturbed LBL cases for Wygnanski and Fiedler (8) and Batt (10): σ_f=9, and the "quiet" LBL case of Liepmann and Laufer (9): σ_f=11.

4) The δ_ω values, evaluated from m_2^{-1} are:

$$\delta_\omega(\text{TBL})/(x-x_o)=0.19,\ \delta_\omega(\text{LBL})/(x-x_o)=0.15 \tag{13}$$

and these values are in the general range of other investigator's results; see Brown and Roshko (1). Their relative magnitude is in agreement with the conclusion of Batt (10), that the TBL case should have a greater spreading rate than the LBL condition.

5) The pronounced differences in m_3^{-1} and m_4^{-1} for both the TBL and LBL conditions suggest that the $\bar{u}/U$ distributions are strongly asymmetric. Consequently, the mean vorticity distribution considered by Dimotakis and Brown (12) is also asymmetric about the y(0.5) location.

Fig. 7a. $\bar{u}/U$ vs $[y-y(.5)]/x$, LBL

Notes: Solid curve is Görtler solution with σ_f defined using m_2. x-locations in cm noted at left. Right side graduations denote 0.05 units of $[y-y(.5)]/x$

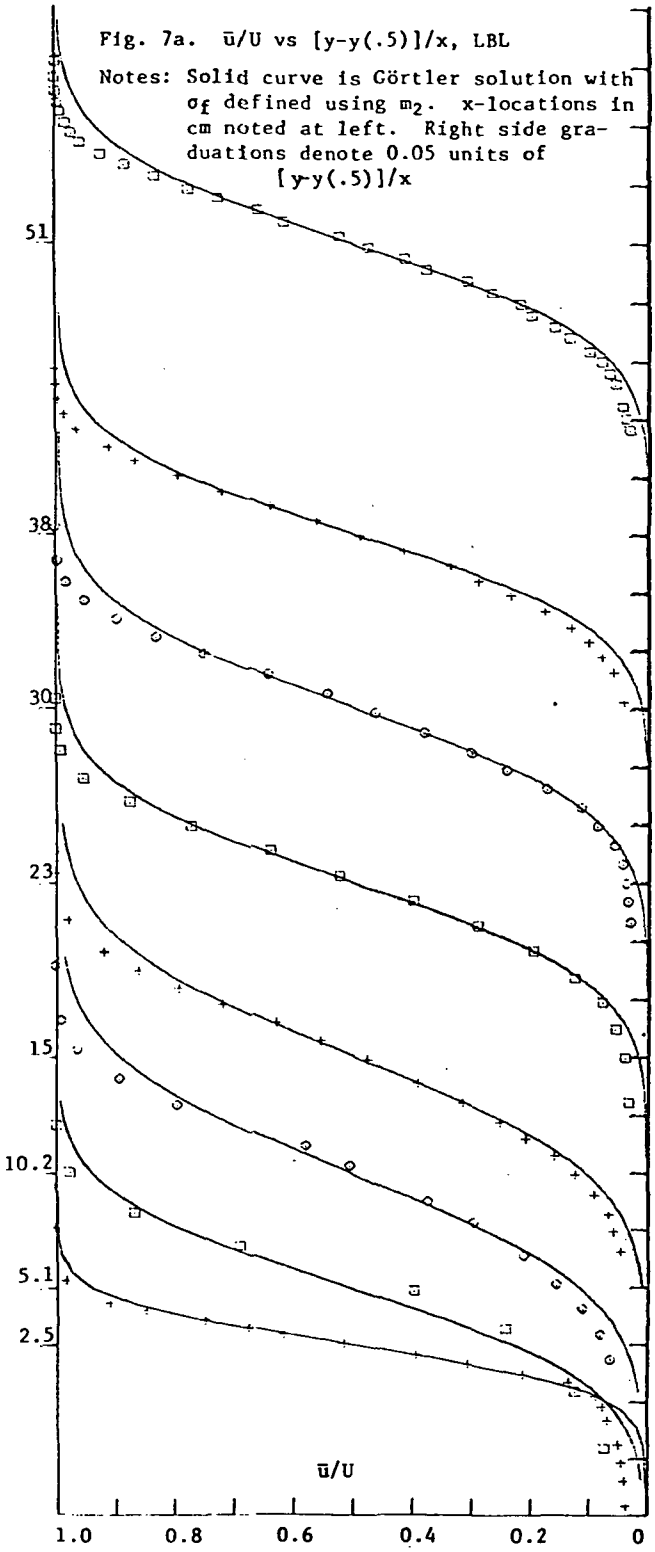

Fig. 7b. $\bar{u}/U$ vs $[y-y(.5)]/x$, TBL

See 7a for explanation of representation

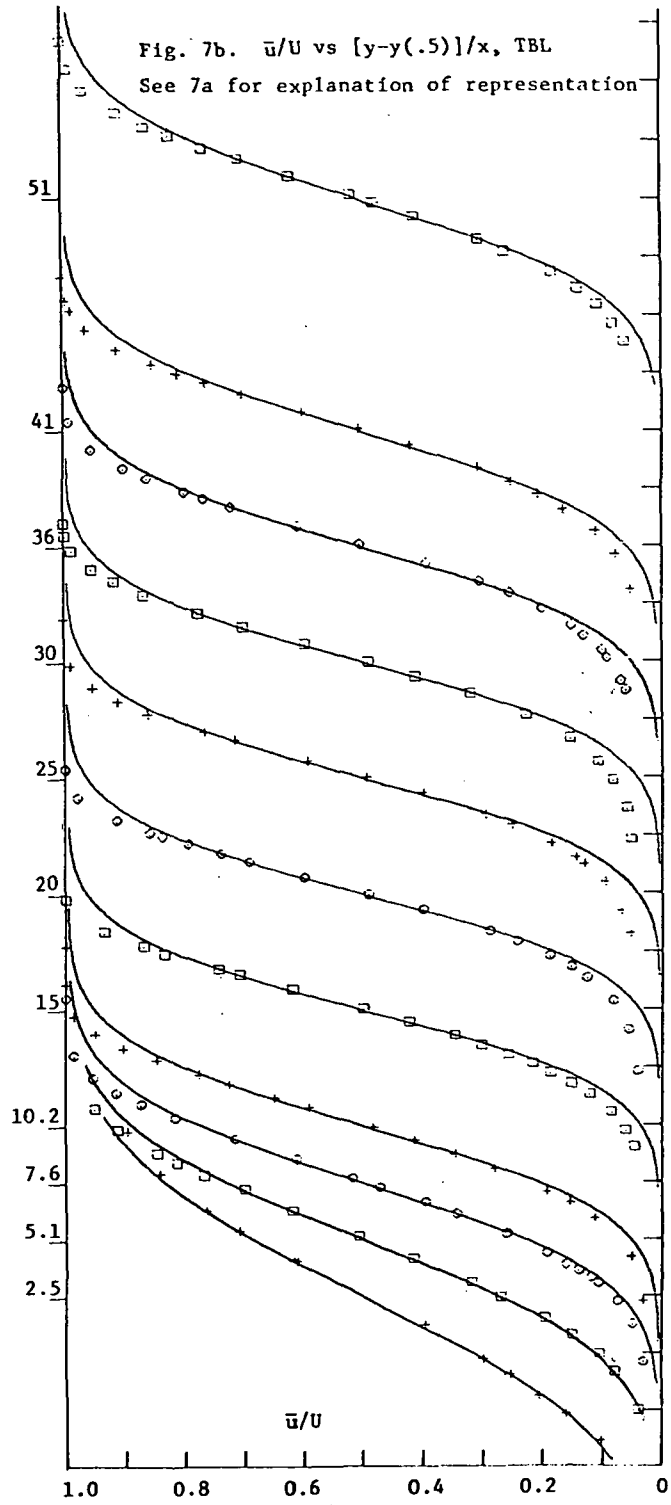

Table 2. Shear layer regions used to define m and S.D. values

Sub	u/U Range	Definition/interpretation
1	$0.1 \le u/U \le 0.99$	Maximum range over which velocity magnitude data approximates $\bar{u}(\bar{v}/\bar{u} \ll 1$ for $\bar{u}/U=0.1)$ and is appropriate for the Gaussian fit $(\bar{u}/U<1.0)$
2	Three maximum u/U values which are <0.5 plus three minimum u/U values which are >0.5	approximation to u/U data which will define the $\partial\bar{u}/\partial y$ at y(0.5)
3	$0.1 \le \bar{u}/U \le 0.6$	low velocity region
4	$0.4 \le \bar{u}/U \le 0.99$	high velocity region

Fig. 8a. $\tilde{u}/U$ vs $[y-y(.5)]/x$, LBL case

Notes: x locations, in cm, of experimental data noted on left side, each mark on right is $\tilde{u}/U=0.05$

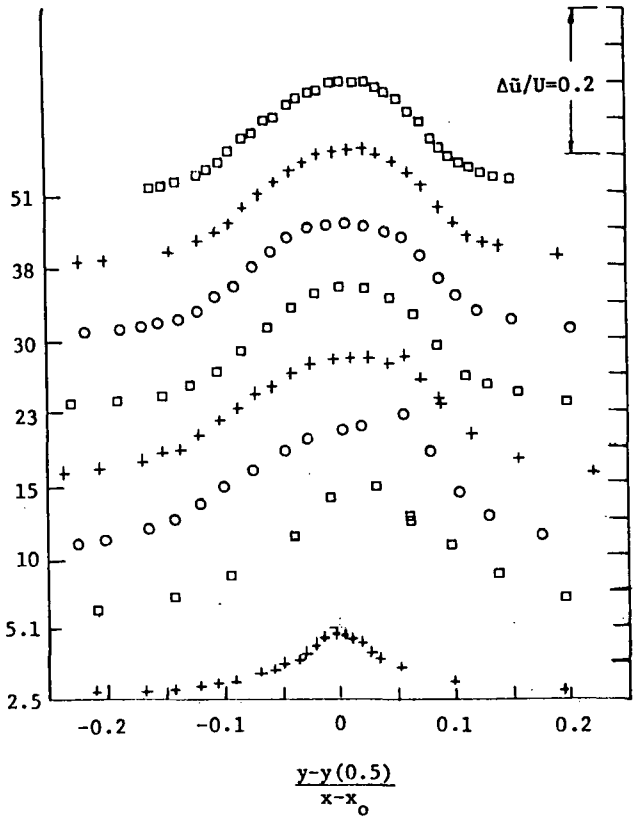

Fig. 8b. $\tilde{u}/U$ vs $[y-y(.5)]/x$, TBL case (see 8a for description of coordinates)

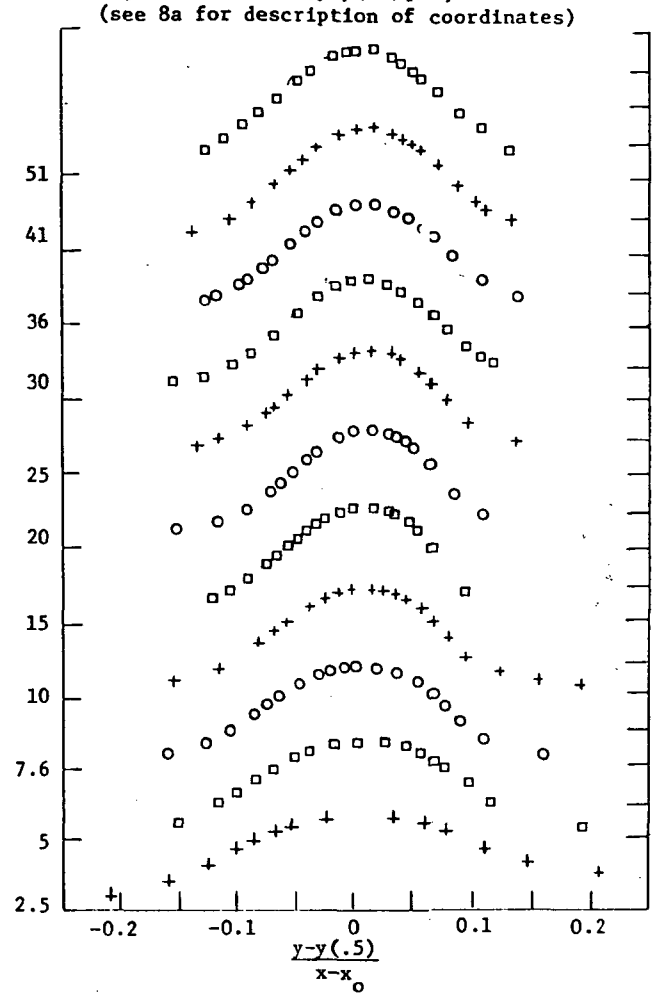

6. The $m^{-1}(x)$ distributions suggest that the development of the LBL and TBL cases are strongly different; the differences are also evident in the $\tilde{u}/U$ vs $[y-y(.5)]/x$ plots of Figure 7. The m^{-1} growth for the LBL case is extremely rapid near x=0 and it appears to reach its final state quite quickly. Conversely, the TBL case exhibits two distinct regions with a clear change in the otherwise constant slope (dm^{-1}/dx) at approximately 25cm or $3000\theta_1$ units. Browand (11) noted a change in the growth rate of his TBL case at $x=(400 \rightarrow 500)\theta_1$ units. It is possible to infer that somewhat similar effects may be present in each flow since the effective time (τ) for the evolution of the layer will be approximately the same for the two conditions. ($\tau \sim x/U_c$ and since $U_c \sim (U_1+U_2)/2$, $\tau(11)/\tau(\text{present}) \simeq (4.5/3)(0.5/0.62) = 1.2$.)

Self-Preservation

The observed linear growth of the shear layer width measure is a necessary, but not a sufficient condition for self-preservation. Other necessary conditions are evaluated below. The maximum $\tilde{u}/U$ value is independent of x for the self-preserving condition; Figure 10 presents the relevant data. This figure shows that the maximum fluctuation intensity distributions are dramatically different for the two cases in the region $0 \leq x \leq 25$cm and that the two seem to be tending toward their asymptotic limits by the end of the measurement region. The constant value $\tilde{u}/U=0.17$ has been added to the plot for visual reference. The apparent difference in the $\tilde{u}/U$ values may be a result of the inadequate averaging time of the r.m.s. voltage value for the LBL vs the TBL data. A more reliable comparison can be based upon the x-dependence of the normalized $\tilde{u}$ values for the separate LBL and TBL cases since the errors within each data set will be constant. This comparison is presented in Figure 11 where the similarity variable $\{[y-y(.5)]/(x-x_o)\}$ is used to evaluate the self-preserving character of the data. A similar representation of the mean velocity data is also presented in Figure 12. These data support the

Table 3 S.D. Values for the $\tilde{u}/U$ regions 1-4

LBL Case (all x100)

x=	2.5	5.1	10	15	23	30	38	51
SD_1	2	2.8	4.3	3.3	2.5	3.6	3.5	3.5
SD_2	0.4	5.4	2.4	0.8	0.7	1.0	0.7	1.0
SD_3	0.9	2.0	1.0	0.5	0.6	0.7	0.6	0.8
SD_4	2.0	0.9	3.9	3.1	2.3	3.2	3.0	2.7

TBL Case (all x100)

2.5	5.1	7.6	10	15	20	25	30	36	41	51
1.4	1.5	3.1	3.5	2.3	2.8	3.7	3.2	2.3	2.9	2.4
0.6	0.7	0.4	0.6	0.5	0.6	0.8	0.7	0.7	0.8	0.6
0.5	0.2	0.4	0.6	0.3	0.9	1.0	1.2	0.9	0.7	0.5
1.1	1.5	2.5	3.2	1.9	2.0	2.9	2.8	1.1	2.2	1.7

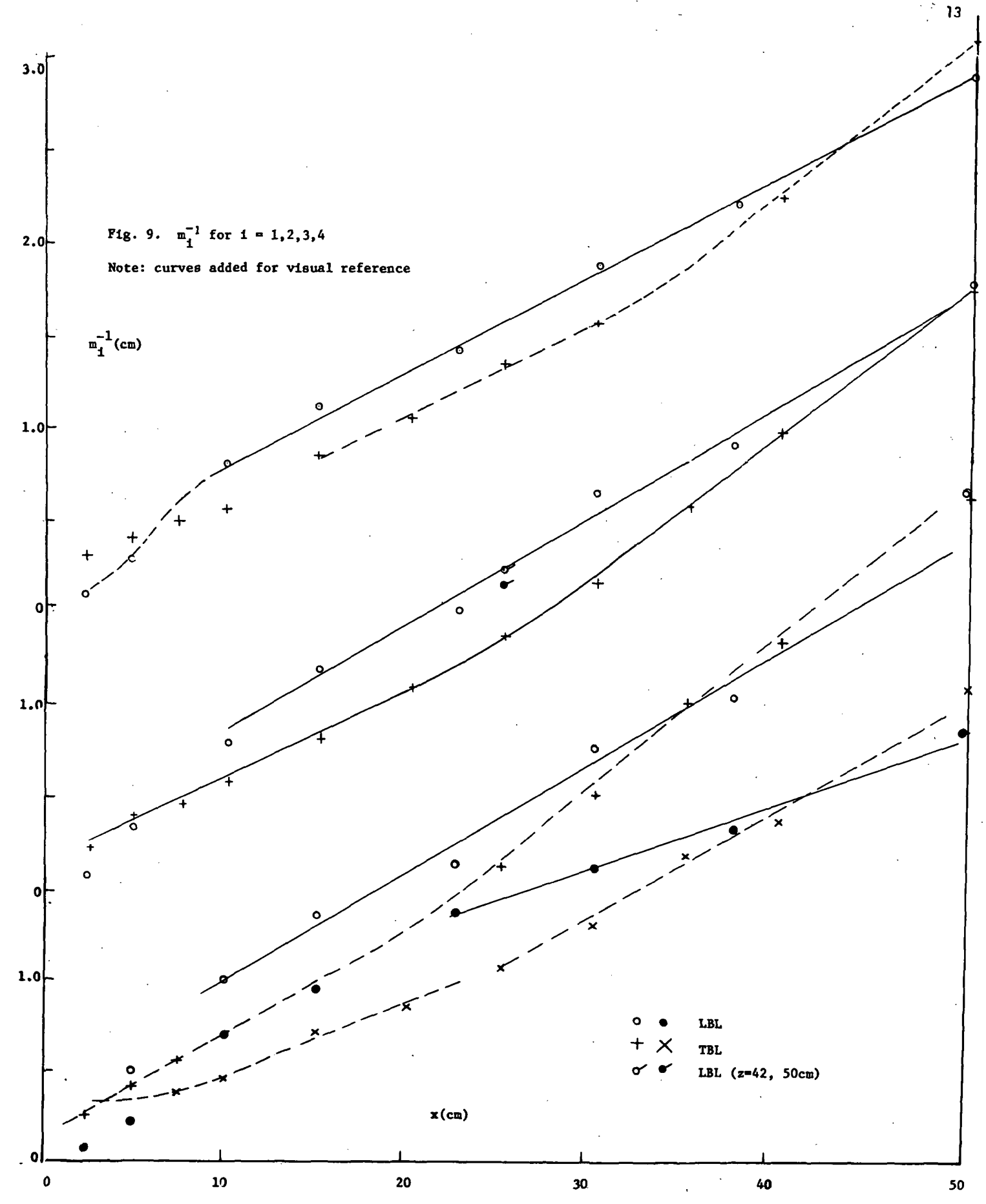

Fig. 9. m_1^{-1} for i = 1,2,3,4

Note: curves added for visual reference

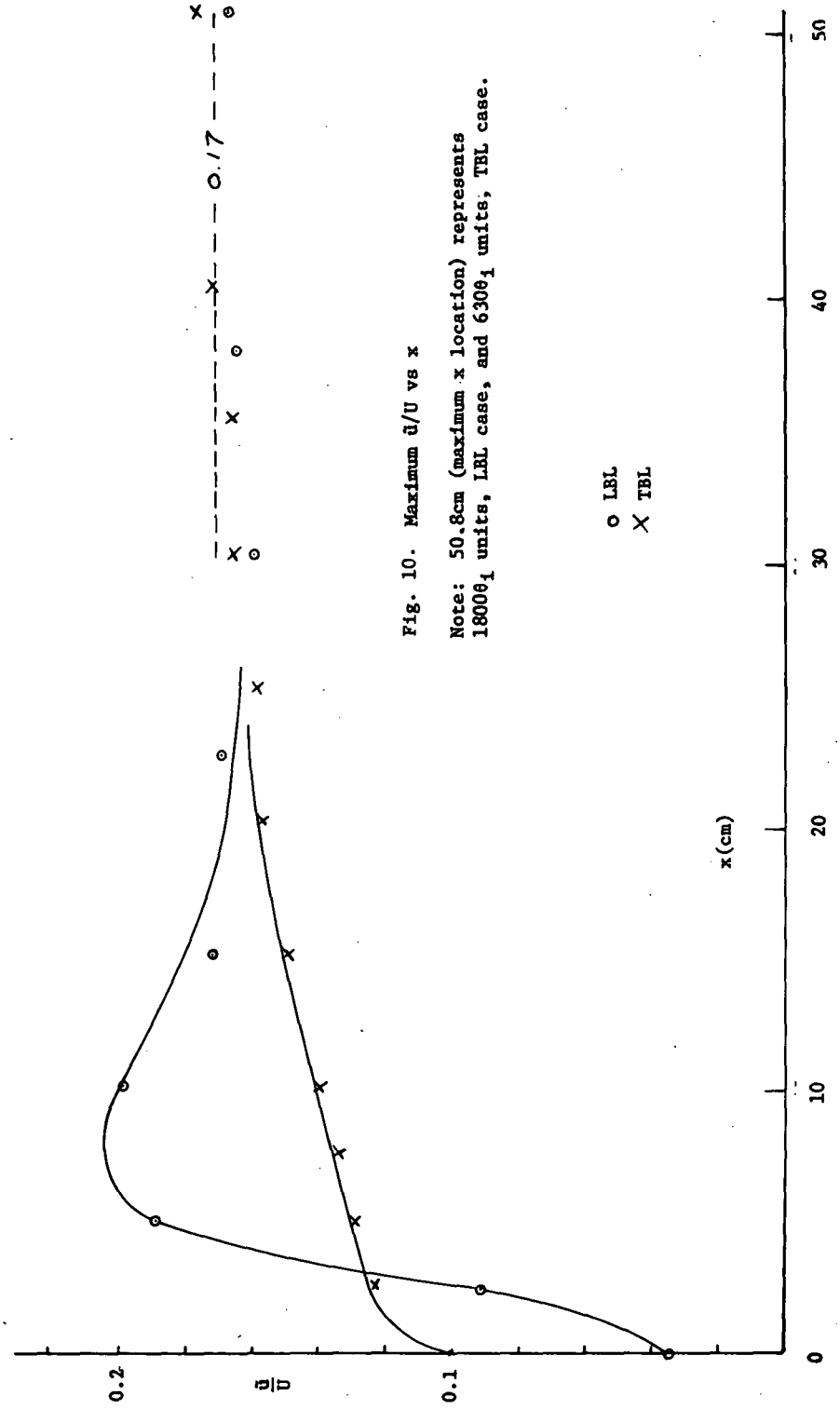

Fig. 10. Maximum ū/U vs x

Note: 50.8cm (maximum x location) represents $1800\theta_1$ units, LBL case, and $6300\theta_1$ units, TBL case.

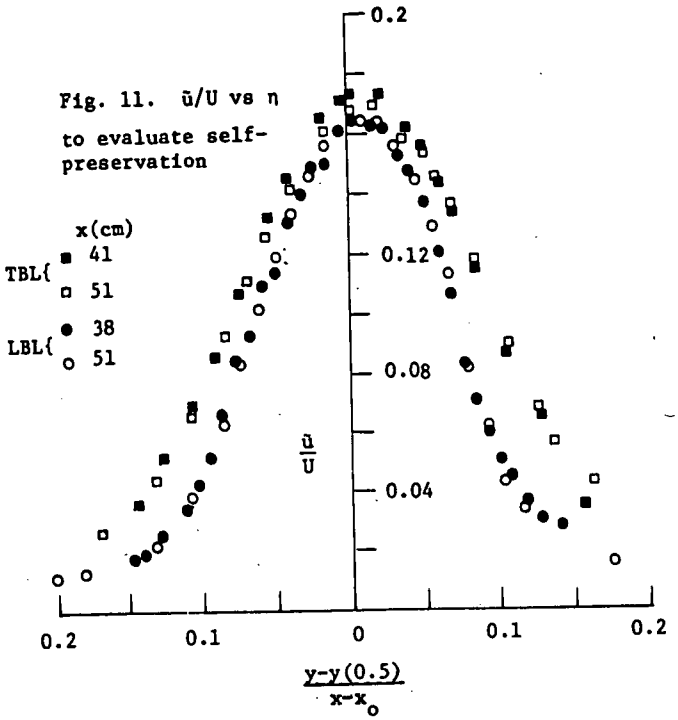

Fig. 11. ū/U vs η to evaluate self-preservation

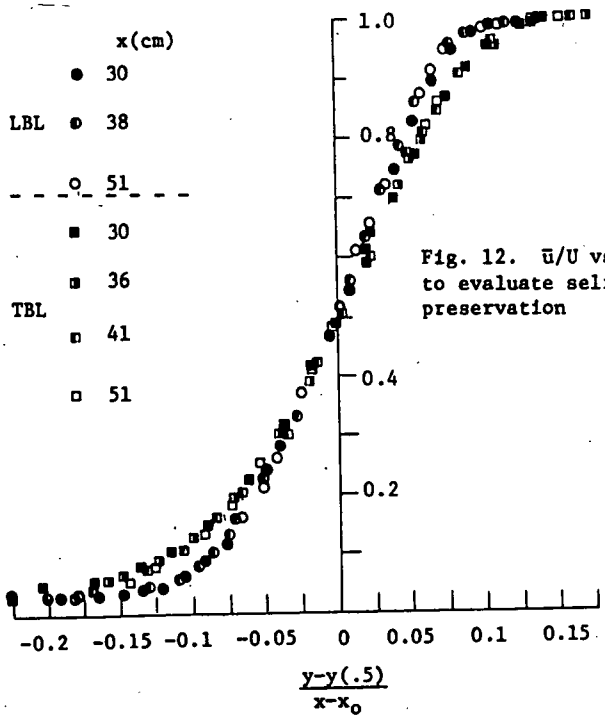

Fig. 12. ū/U vs η to evaluate self-preservation

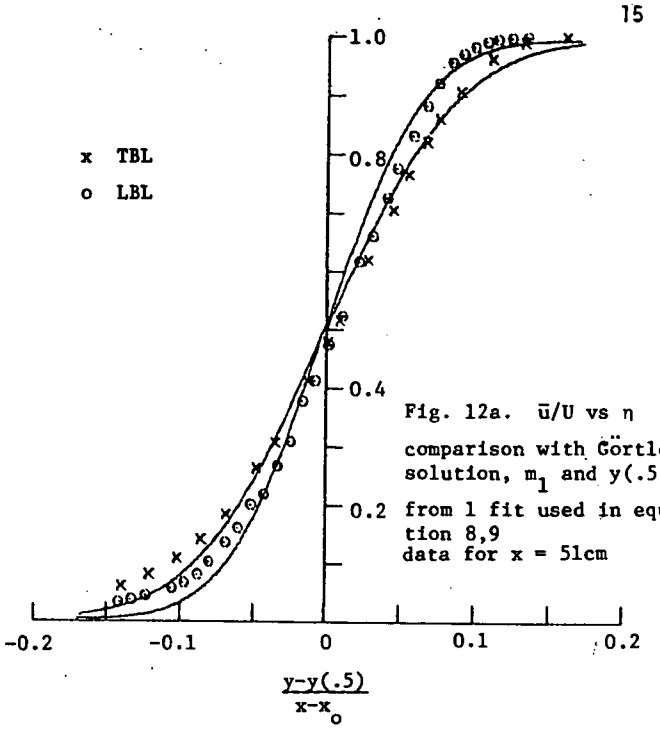

Fig. 12a. ū/U vs η comparison with Görtler solution, m_1 and y(.5) from 1 fit used in equation 8,9 data for x = 51cm

interpretation that the flow has become self-preserving by $Re_x=6.7x10^5$ and that the turbulent boundary layer initial condition does result in a wider mixing layer. The ū values can also be compared with the ũ data summarized by Champagne et. al. (11). The present data have been added to the plot taken directly from this reference; see Figure 13. A very close agreement between the TBL case and that of the Patel (13) and Champagne et. al. (11) studies is evident. The LBL data appear to be in agreement with the Liepmann and Laufer (8) results with the exception of the maximum ũ values for the present data.

Interpretation of the TBL and LBL Initial Condition Effects

The laminar/turbulent state of the boundary layer at x=0 clearly has a significant effect on the initial development of the plane mixing layer; the streamwise evolution of the fluctuation intensity and the mean velocity distributions are quite different for the two cases. The TBL case shows a pronounced change in its characteristics at $x/\theta_1 \simeq 300$ or 25cm whereas the LBL case is not similarly differentiated except for the ũ/U maximum values.

The quite interesting question about the initial condition effects on the asymptotic state cannot be definitively answered with these data; however, the data comparisons which involve the similarity coordinate $\{[y-y(.5)]/(x-x_o)\}$ do support the proposition that the effects persist in the region of self-preservation.

The present study is, however, not constrained to simply form comparative evaluations using the similarity coordinates. Since the same apparatus and the "same" flow speed* and streamwise locations were used for the measurements, a direct comparison of the experimental data is possible. The ū and ũ data for

*U(LBL) = 18.59mps = 1.02 U(TBL)

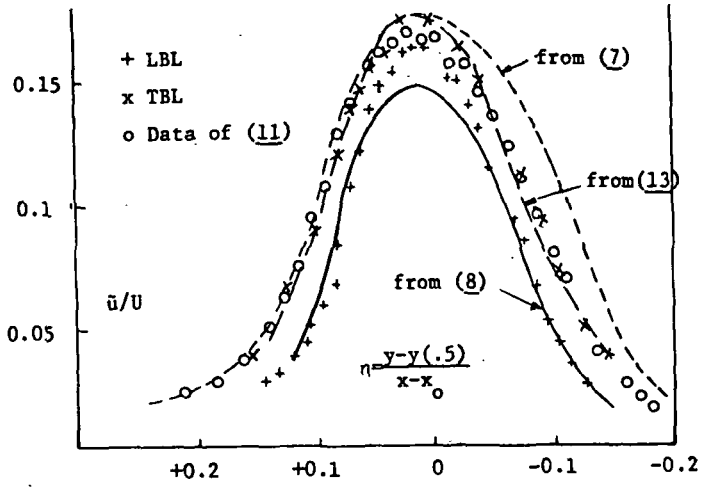

Fig. 13 ũ/U vs η

Note original curve with (7), (8) and (13) data points added to original data of (11) taken directly from reference (11). Present data added to plot with ũ/U<0.5 for η>0 convention of (11).

x=50.8cm are presented in Figure 14. This representation of the data provides a very strong contradiction to the earlier inferred influence of the initial conditions ... the flow fields from both the laminar and the turbulent initial conditions are essentially identical.*

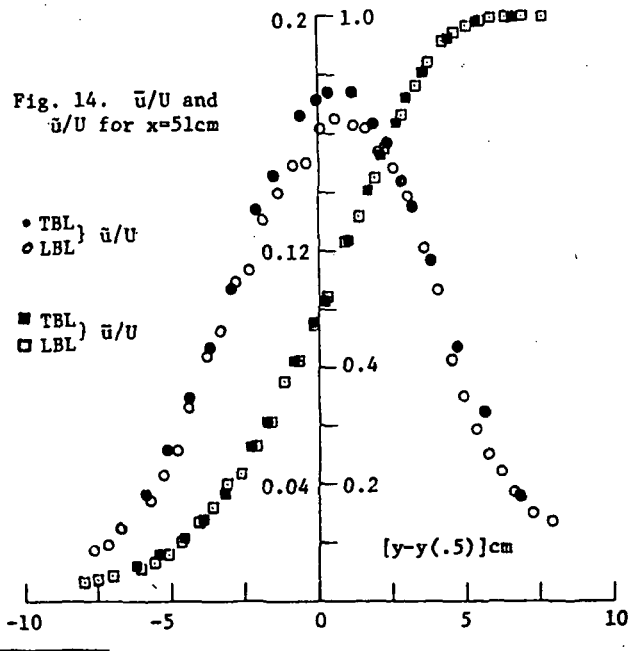

Fig. 14. ū/U and ũ/U for x=51cm

*The maximum r.m.s. fluctuation level at x=50.8cm was rechecked to evaluate the possible influence of an insufficient averaging time for the LBL case data. Several long term (30 sec.) analog voltage signals ẽ were collected for both the LBL and TBL cases. These results confirmed that the ũ/U distribution for the TBL case was slightly wider but the amplitude difference was reduced to ≈3%. Maximum ũ values were ũ/U(TBL)=0.185 and ũ/U(LBL)=0.18.

With this insight, it is not difficult to reevaluate the earlier evidence which seemed to suggest a continuing effect of the initial condition. Specifically, if one combines the self-preserving condition: dl/dx= constant (where l is a width measure of the shear layer), with the observation that a derivative is best evaluated from experimental data if the largest possible span of the independent variable is utilized, the use of x_o in the expression for the similarity variable is logical and evaluating it from an upstream extrapolation of the available data is reasonable. However, this commonly accepted procedure is not easily adapted to a situation where the x derivative of l ... in this case dm_2^{-1}/dx ... only slowly approaches its asymptotic value. By inference, this is the actual situation for the m_2^{-1} of, at least, the LBL case although it is too subtle an effect to be evident from Figure 9. The earlier quoted observation of Dimotakis and Brown (12) that ... the growth rate $d\delta_\omega/dx$ depends upon the vorticity distribution which is, in turn, related to δ_ω ... is quite useful in recognizing the cause for the gradual change in the m_2^{-1} slope for the LBL case. It is interesting to speculate on the reason for the apparent differences in the "time" to achieve an asymptotic state for the two initial boundary layer conditions. A related point of interest can be identified by comparing the tripped LBL data, e.g. (9), (11), with the present LBL and TBL cases. Such a comparison suggests that the character of the disturbance, and not its amplitude, is responsible for the substantial effect on the x_o inferred from the ū(x,y) in the developing region. (Note that $m_2^{-1}(x=25, z=42) \approx m_2^{-1}(x=25, z=71)$ see Fig. 9 and ũ(o,y,42)(max-LBL) = 3 ũ(o,y,71)(max-LBL) = 1.2 ũ(o,y,71)(max-TBL).)

The suggestion that is often made: that a quite large Re_x is required to observe a self-preserving condition, can be interpreted in the context of the present measurements. It is clear from an examination of Figure 9 that a large increase in the x values would be required to infer the same x_o for the LBL and TBL cases. Conversely, if a self-preserving flow is one in which the effects of the initial condition are lost, and if an experimental program which allows the two states to be obtained in the same apparatus is executed, then a certain determination that self-preservation has been obtained will result from "identical" ū and ũ distributions. An added benefit is that the necessary Re_x value will be significantly smaller than that which would be required if the x_o value were to be precisely defined by the upstream extrapolation of l(x).

SUMMARY

Data to document the developing region of a plane mixing layer have been acquired for the two distinct initial conditions: a laminar and a turbulent boundary layer at x=0.

The initial development of these two flow fields is dramatically different; it is proposed that these data will constitute a viable reference case for the evaluation of calculation schemes.

The question of the initial condition effects on the self-preserving mixing layer has been addressed. It is proposed, on the basis of these data, that the initial condition is not relevant in the self-preserving state and that the apparent influence is a consequence of using an inappropriately evaluated similarity variable. The present data, when interpreted in the standard manner, reveal that the misinterpretation is quite easily made and that the correct evaluation requires the inference of very subtle changes in the slope of the width measure's x-dependence.

ACKNOWLEDGEMENTS

Personal gratitude is expressed to Mr. Curtis Monroe, programmer, Ms. Mary Grace, typist, Mr. Frank Walker, draftsman and Mr. Dave Sigmon, electronics technician. The financial support of the High-Speed Aerodynamics Division of the NASA Langley Research Center, Mr. Michael Fischer and Mr. Jerry Heffner, grant monitors, and the Division of Engineering Research, MSU, Mr. J.W. Hoffman, Director, is gratefully acknowledged.

REFERENCES

1 Brown, G.L. and Roshko, A., "On Density Effects and Large Structure in Turbulent Mixing Layers," Journal of Fluid Mechanics, Vol. 64, Part 4, 1974, pp. 775-816.

2 Winant, C.D. and Browand, F.K., "Vortex Pairing: The Mechanism of Turbulent Mixing-layer Growth at Moderate Reynolds Number," Journal of Fluid Mechanics, Vol. 63, Part 2, Jan. 1974, pp. 237-255.

3 , "Free Turbulent Shear Flows, Vol. 1," Conference Proceedings, NASA SP-321, July 1972.

4 Murthy, S.N.B. (ed.), Turbulent Mixing in Non-Reactive and Reactive Flows, Plenum Press, New York, 1975.

5 Townsend, A.A., The Structure of Turbulent Shear Flow, 2nd Ed., Cambridge U. Press, Cambridge, 1976.

6 Bradshaw, P., "The Effect of Initial Conditions on the Development of a Free Shear Layer," Journal of Fluid Mechanics, Vol. 26, Part 2, 1966, pp. 225-236.

7 Wygnanski, I. and Fiedler, H.E., "The Two-Dimensional Mixing Region," Journal of Fluid Mechanics, Vol. 41, Part 2, April 1970, pp. 327-361.

8 Liepmann, H.W. and Laufer, Jr., "Investigations of Free Turbulent Mixing," NACA Report No. 1257, 1947.

9 Batt, R.G., "Some Measurements on the Effect of Tripping the Two-Dimensional Shear Layer," AIAA Journal, Vol. 13, No. 2, Feb. 1975, pp. 245-246.

10 Browand, F.K., "The Effect of Initial Conditions Upon the Growth of the Two-Dimensional Mixing Layer," APS Bulletin, Series II, Vol. 21, No. 10, Nov. 1976, p. 1221.

11 Champagne, F.H., Pao, Y.H. and Wygnanski, I. J., "On the Two-Dimensional Mixing Region," Journal of Fluid Mechanics, Vol. 74, Part 2, 1976, pp. 209-250.

12 Dimotakis, P.E. and Brown, G.L., "Large Structure Dynamics and Entrainment in the Mixing Layer at High Reynolds Number," Project SQUID Technical Report CIT-7-PU, August 1975.

13 Patel, R.P., "An Experimental Study of a Plane Mixing Layer," AIAA Journal, Vol. 11, No. 1, Jan. 1973, pp. 67-71.

14 Chevray, R. and Kovasznay, L.S.G., "Turbulence Measurements in the Wake of a Thin Flat Plate," AIAA Journal, Vol. 7, No. 8, 1969, pp. 1641-1643.

15 Comte-Bellot, G., Strohl, A. and Alcaraz, E., "On Aerodynamic Disturbances Caused by Single Hot-Wire Probes," Journal of Applied Mechanics, Vol. 38, Trans. ASME, Vol. 93, E, Dec. 1971, pp. 767-774.

16 Brunn, H.H., "Interpretation of a Hot Wire Signal Using a Universal Calibration Law," Journal of Phys. E., Sci. Instr., Vol. 4, 1971, pp. 225-231.

17 Coles, D., "The Turbulent Boundary Layer in a Compressible Fluid, Rand Report, R-403-PR, 1962.

18 Clauser, F.H., "Turbulent Boundary Layers in Adverse Pressure Gradients," Jour. Aero. Sci., Vol. 21, 1954, pp. 91-108.

19 Görtler, H., "Berechnung von Aufgaven der freien Turbulenz auf Grund eines neuen Naherungsansatzes, Z. Anger. Math. Mech., Bd. 22, Nr. 5, Oct. 1942, pp. 244-254.

Appendix B

Tabulation of the Boundary Shear Layer Data

Note: The boundary layer parameters computed from these data are presented in Table 1.
The m and y(0.5) values associated with the shear layer traverses are taken from the number 2 fitted region; see Table 2.

T.B.L. 1/22/77 x= 0.00 cm

y(cm)	U/Umax	U'/Umax
0.001	0.139	0.046
0.011	0.246	0.066
0.024	0.478	0.103
0.034	0.570	0.099
0.039	0.610	0.094
0.052	0.637	0.090
0.110	0.729	0.074
0.166	0.773	0.070
0.207	0.804	0.068
0.263	0.839	0.064
0.296	0.857	0.062
0.344	0.880	0.058
0.387	0.899	0.055
0.438	0.920	0.052
0.489	0.938	0.047
0.530	0.950	0.043
0.570	0.963	0.038
0.603	0.970	0.033
0.649	0.977	0.029
0.895	0.992	0.006
1.066	1.000	0.000

Umax ..... 18.250 mps
DeltaD ..... 0.116 cm
Theta ..... 0.081 cm
Umax*Theta/Nu 1061.

L.B.L. 1/8/77 x= 0.00 cm

y(cm)	U/Umax	U'/Umax
0.023	0.251	0.017
0.030	0.335	0.020
0.038	0.406	0.023
0.058	0.559	0.029
0.071	0.635	0.030
0.084	0.698	0.030
0.099	0.756	0.033
0.099	0.760	0.030
0.109	0.800	0.030
0.130	0.878	0.027
0.152	0.937	0.022
0.183	0.978	0.014
0.203	0.991	0.009
0.269	1.000	0.003
0.310	0.998	0.001
0.737	0.994	0.001
0.996	0.993	0.001

Umax ..... 18.690 mps
DeltaD ..... 0.067 cm
Theta ..... 0.031 cm
Umax*Theta/Nu 416.

Boundary Layer data taken with shear layer traverses z = 71cm

L.B.L. 1/2/77 x= 0.00 cm
z=20.00 cm

y(cm)	U/Umax	U'/Umax
0.005	0.150	0.012
0.015	0.309	0.024
0.023	0.362	0.027
0.036	0.464	0.031
0.046	0.548	0.034
0.061	0.647	0.042
0.086	0.775	0.040
0.104	0.853	0.039
0.127	0.917	0.033
0.152	0.961	0.026
0.178	0.983	0.014
0.201	0.993	0.008
0.226	0.998	0.003
0.259	0.999	0.004
0.292	1.000	0.003
0.414	0.997	0.003
0.513	0.996	0.003

Umax ..... 18.270 mps
DeltaD ..... 0.053 cm
Theta ..... 0.026 cm
Umax*Theta/Nu 341.

L.B.L. 1/2/77 x= 0.00 cm
z=50.00 cm

y(cm)	U/Umax	U'/Umax
0.010	0.159	0.010
0.015	0.225	0.015
0.025	0.309	0.019
0.041	0.433	0.026
0.056	0.549	0.032
0.074	0.647	0.032
0.091	0.761	0.035
0.112	0.855	0.032
0.145	0.943	0.021
0.170	0.974	0.013
0.198	0.992	0.006
0.226	0.999	0.003
0.257	1.000	0.003
0.284	1.000	0.003
0.315	0.999	0.003
0.409	0.998	0.003
0.521	0.997	0.003

Umax ..... 18.250 mps
DeltaD ..... 0.060 cm
Theta ..... 0.027 cm
Umax*Theta/Nu 354.

L.B.L. 1/2/77 x= 0.00 cm
z=42.00 cm

y(cm)	U/Umax	U'/Umax
0.008	0.201	0.043
0.015	0.314	0.063
0.028	0.420	0.083
0.041	0.490	0.093
0.061	0.622	0.117
0.074	0.710	0.112
0.091	0.783	0.114
0.112	0.845	0.113
0.137	0.904	0.100
0.173	0.951	0.073
0.206	0.981	0.050
0.241	0.990	0.034
0.284	0.997	0.024
0.333	0.999	0.015
0.384	1.000	0.006
0.460	0.998	0.005
0.516	0.999	0.004

Umax ..... 18.270 mps
DeltaD ..... 0.057 cm
Theta ..... 0.029 cm
Umax*Theta/Nu 380.

L.B.L. 1/2/77 x= 0.00 cm
z=58.00 cm

y(cm)	U/Umax	U'/Umax
0.015	0.142	0.016
0.023	0.193	0.023
0.030	0.249	0.030
0.041	0.336	0.041
0.058	0.462	0.050
0.071	0.548	0.060
0.086	0.643	0.061
0.104	0.730	0.066
0.124	0.821	0.069
0.152	0.899	0.054
0.178	0.943	0.042
0.201	0.972	0.030
0.234	0.989	0.022
0.272	0.997	0.006
0.312	0.999	0.004
0.391	1.000	0.003
0.516	0.998	0.003

Umax ..... 18.260 mps
DeltaD ..... 0.075 cm
Theta ..... 0.031 cm
Umax*Theta/Nu 406.

L.B.L. 1/2/77 x= 0.00 cm
z=71.00 cm

y(cm)	U/Umax	U'/Umax
0.020	0.226	0.014
0.041	0.386	0.024
0.058	0.520	0.028
0.091	0.713	0.033
0.114	0.823	0.032
0.137	0.894	0.028
0.163	0.951	0.022
0.196	0.986	0.009
0.231	0.996	0.005
0.259	1.000	0.003
0.295	1.000	0.003
0.361	0.998	0.003
0.493	0.997	0.003

Umax ..... 18.290 mps
DeltaD ..... 0.067 cm
Theta ..... 0.028 cm
Umax*Theta/Nu 367.

L.B.L. 1/2/77 x= 0.00 cm
z=86.00 cm

y(cm)	U/Umax	U'/Umax
0.010	0.149	0.015
0.018	0.212	0.022
0.028	0.300	0.030
0.041	0.405	0.042
0.056	0.525	0.047
0.079	0.651	0.058
0.094	0.736	0.062
0.117	0.833	0.056
0.142	0.909	0.055
0.168	0.958	0.038
0.196	0.982	0.031
0.221	0.992	0.026
0.241	0.997	0.017
0.302	1.000	0.006
0.348	0.999	0.004
0.414	0.998	0.003
0.470	0.998	0.003

Umax ..... 18.260 mps
DeltaD ..... 0.065 cm
Theta ..... 0.029 cm
Umax*Theta/Nu 380.

T.B.L. 1/4/77 x= 0.00 cm
z=50.00 cm

y(cm)	U/Umax	U'/Umax
0.020	0.455	0.031
0.033	0.582	0.099
0.056	0.665	0.089
0.089	0.723	0.078
0.117	0.754	0.074
0.155	0.785	0.071
0.193	0.816	0.068
0.234	0.841	0.067
0.272	0.867	0.063
0.317	0.891	0.061
0.373	0.915	0.057
0.439	0.943	0.051
0.498	0.962	0.044
0.521	0.964	0.042
0.564	0.979	0.034
0.627	0.989	0.027
0.650	0.990	0.026
0.658	0.988	0.026
0.787	0.996	0.012
0.922	0.999	0.004
1.036	1.000	0.003
1.135	0.999	0.003
1.232	0.998	0.003
1.333	0.998	0.003

Umax ..... 18.370 mps
DeltaD ..... 0.100 cm
Theta ..... 0.069 cm
Umax*Theta/Nu 910.

T.B.L. 1/4/77 x= 0.00 cm
z=42.00 cm

y(cm)	U/Umax	U'/Umax
0.005	0.307	0.028
0.010	0.467	0.032
0.028	0.592	0.098
0.043	0.638	0.092
0.066	0.683	0.085
0.099	0.721	0.080
0.130	0.742	0.077
0.165	0.768	0.074
0.211	0.792	0.072
0.246	0.807	0.071
0.287	0.827	0.070
0.325	0.844	0.068
0.363	0.851	0.066
0.411	0.869	0.064
0.460	0.884	0.063
0.516	0.897	0.061
0.577	0.917	0.058
0.630	0.929	0.056
0.686	0.937	0.053
0.770	0.955	0.048
0.828	0.965	0.043
0.892	0.975	0.037
0.925	0.980	0.034
1.003	0.991	0.026
1.077	0.996	0.017
1.153	0.998	0.009
1.247	1.000	0.005
1.341	1.000	0.003

Umax ..... 18.370 mps
DeltaD ..... 0.137 cm
Theta ..... 0.104 cm
Umax*Theta/Nu 1371.

T.B.L. 1/4/77 x= 0.00 cm
z=58.00 cm

y(cm)	U/Umax	U'/Umax
0.018	0.395	0.028
0.036	0.533	0.099
0.071	0.676	0.084
0.109	0.728	0.076
0.150	0.764	0.072
0.180	0.787	0.070
0.211	0.806	0.068
0.241	0.824	0.066
0.282	0.849	0.063
0.335	0.874	0.060
0.394	0.901	0.057
0.442	0.916	0.054
0.503	0.941	0.049
0.566	0.958	0.043
0.635	0.973	0.036
0.706	0.985	0.029
0.762	0.991	0.023
0.831	0.995	0.015
0.894	0.998	0.008
0.950	1.000	0.005
1.021	0.999	0.004
1.059	1.000	0.004
1.168	1.000	0.003
1.260	0.999	0.003

Umax ..... 18.380 mps
DeltaD ..... 0.116 cm
Theta ..... 0.079 cm
Umax*Theta/Nu 1042.

T.B.L. 1/4/77 x= 0.00 cm
z=71.00 cm

y(cm)	U/Umax	U'/Umax
0.013	0.345	0.028
0.030	0.495	0.032
0.061	0.645	0.090
0.097	0.707	0.079
0.137	0.744	0.074
0.175	0.771	0.071
0.218	0.797	0.069
0.269	0.829	0.065
0.325	0.855	0.062
0.450	0.899	0.056
0.516	0.921	0.052
0.584	0.944	0.048
0.655	0.958	0.043
0.714	0.970	0.038
0.780	0.983	0.029
0.843	0.988	0.026
0.907	0.994	0.016
0.973	0.997	0.011
1.041	1.000	0.006
1.135	1.000	0.003
1.229	1.000	0.003
1.326	0.999	0.003

Umax ..... 18.350 mps
DeltaD ..... 0.129 cm
Theta ..... 0.090 cm
Umax*Theta/Nu 1185.

L.B.L. 1/8/77 x= 2.54 cm Umax=18.61 mps

y(cm)	(y-y(.5))/x	U/Umax	U'/Umax
-5.596	-2.219	0.034	0.006
-3.614	-1.439	0.031	0.005
-2.548	-1.019	0.031	0.005
-1.598	-0.645	0.030	0.005
-1.275	-0.518	0.030	0.006
-1.029	-0.421	0.031	0.005
-0.767	-0.318	0.026	0.005
-0.485	-0.207	0.029	0.008
-0.378	-0.165	0.031	0.011
-0.317	-0.141	0.035	0.014
-0.262	-0.119	0.039	0.018
-0.221	-0.103	0.043	0.021
-0.221	-0.103	0.044	0.021
-0.180	-0.087	0.049	0.025
-0.127	-0.066	0.066	0.035
-0.097	-0.054	0.075	0.040
-0.074	-0.045	0.087	0.047
-0.043	-0.033	0.134	0.053
-0.025	-0.026	0.211	0.062
-0.003	-0.017	0.305	0.074
0.018	-0.009	0.392	0.086
0.043	0.001	0.514	0.092
0.063	0.009	0.617	0.091
0.079	0.015	0.675	0.083
0.097	0.022	0.748	0.076
0.117	0.030	0.847	0.061
0.135	0.037	0.909	0.053
0.183	0.056	0.983	0.042
0.300	0.102	1.000	0.022
0.544	0.198	0.997	0.008
0.843	0.316	0.996	0.002
1.247	0.475	0.996	0.001
1.829	0.704	0.995	0.001

z=m*y+b; 1/m=0.081 cm; y(.5)=-b/m= 0.040 cm

L.B.L. 1/8/77 x= 5.08 cm Umax=18.49 mps

y(cm)	(y-y(.5))/x	U/Umax	U'/Umax
-7.526	-1.449	0.031	0.006
-5.707	-1.091	0.036	0.005
-5.596	-1.069	0.037	0.005
-3.739	-0.704	0.034	0.006
-2.791	-0.517	0.040	0.005
-2.233	-0.407	0.042	0.007
-1.727	-0.308	0.044	0.010
-1.212	-0.206	0.053	0.020
-0.876	-0.140	0.073	0.038
-0.625	-0.091	0.123	0.068
-0.345	-0.036	0.240	0.120
-0.178	-0.003	0.396	0.175
0.023	0.037	0.688	0.189
0.170	0.066	0.867	0.148
0.170	0.066	0.868	0.141
0.348	0.101	0.975	0.108
0.554	0.141	0.998	0.067
0.851	0.200	0.996	0.034
1.115	0.252	0.997	0.017
1.450	0.318	0.996	0.005
1.786	0.384	0.996	0.003
2.553	0.535	0.996	0.003
4.150	0.849	0.996	0.003
6.215	1.256	1.000	0.003

z=m*y+b; 1/m=0.329 cm; y(.5)=-b/m=-0.164 cm

L.B.L. 1/8/77 x=10.16 cm Umax=18.57 mps

y(cm)	(y-y(.5))/x	U/Umax	U'/Umax
-7.668	-0.719	0.033	0.006
-5.596	-0.515	0.037	0.007
-3.632	-0.322	0.038	0.010
-2.979	-0.258	0.038	0.015
-2.979	-0.258	0.038	0.015
-2.977	-0.257	0.038	0.014
-2.626	-0.223	0.043	0.021
-2.395	-0.200	0.048	0.026
-2.014	-0.163	0.063	0.042
-1.791	-0.141	0.080	0.055
-1.565	-0.118	0.110	0.076
-1.346	-0.097	0.155	0.099
-1.097	-0.072	0.211	0.122
-0.800	-0.043	0.296	0.147
-0.615	-0.025	0.374	0.164
-0.297	0.006	0.505	0.178
-0.124	0.023	0.580	0.182
0.244	0.060	0.794	0.198
0.478	0.083	0.892	0.148
0.732	0.108	0.963	0.089
0.983	0.132	0.990	0.057
1.453	0.179	1.000	0.029
2.383	0.270	0.997	0.006
4.254	0.454	0.997	0.003
6.215	0.647	0.997	0.003

z=m*y+b; 1/m=0.827 cm; y(.5)=-b/m=-0.362 cm

L.B.L. 1/8/77 x=15.24 cm Umax=18.67 mps

y(cm)	(y-y(.5))/x	U/Umax	U'/Umax
-7.145	-0.431	0.030	0.006
-5.154	-0.300	0.033	0.011
-4.633	-0.266	0.035	0.012
-4.173	-0.236	0.034	0.015
-3.696	-0.204	0.038	0.020
-3.167	-0.170	0.047	0.030
-2.898	-0.152	0.059	0.042
-2.672	-0.137	0.069	0.047
-2.418	-0.120	0.093	0.065
-2.146	-0.103	0.126	0.085
-1.900	-0.086	0.161	0.102
-1.671	-0.071	0.210	0.121
-1.450	-0.057	0.254	0.132
-1.194	-0.040	0.318	0.150
-0.937	-0.023	0.393	0.162
-0.622	-0.003	0.478	0.169
-0.378	0.013	0.557	0.171
-0.145	0.029	0.633	0.169
0.112	0.046	0.720	0.161
0.323	0.059	0.794	0.172
0.549	0.074	0.862	0.139
0.792	0.090	0.920	0.114
0.805	0.091	0.921	0.107
1.204	0.117	0.980	0.065
1.814	0.157	1.000	0.030
2.786	0.221	0.998	0.011
4.247	0.317	0.999	0.004

z=m*y+b; 1/m=1.220 cm; y(.5)=-b/m=-0.582 cm

L.B.L. 1/8/77 x=22.86 cm Umax=18.68 mps

y(cm)	$\frac{y-y(.5)}{x}$	$\frac{U}{Umax}$	$\frac{U'}{Umax}$
-7.206	-0.280	0.031	0.009
-6.040	-0.229	0.035	0.012
-5.123	-0.189	0.034	0.015
-4.234	-0.150	0.040	0.022
-3.673	-0.126	0.057	0.037
-3.150	-0.103	0.080	0.055
-2.677	-0.082	0.128	0.082
-2.149	-0.059	0.199	0.115
-1.648	-0.037	0.292	0.142
-1.171	-0.016	0.400	0.160
-0.678	0.005	0.525	0.169
-0.183	0.027	0.642	0.167
0.325	0.049	0.773	0.153
0.790	0.069	0.876	0.130
1.257	0.090	0.955	0.087
1.793	0.113	0.992	0.046
2.220	0.132	0.999	0.034
2.809	0.158	1.000	0.023
3.785	0.200	0.999	0.009
6.353	0.313	0.999	0.003

z=m*y+b; 1/m=1.534 cm; y(.5)=-b/m=-0.797 cm

L.B.L. 1/8/77 x=30.48 cm Umax=18.65 mps

y(cm)	$\frac{y-y(.5)}{x}$	$\frac{U}{Umax}$	$\frac{U'}{Umax}$
-8.786	-0.254	0.033	0.012
-7.582	-0.215	0.031	0.013
-6.673	-0.185	0.032	0.016
-6.121	-0.167	0.037	0.019
-5.651	-0.152	0.040	0.023
-5.149	-0.135	0.046	0.029
-4.658	-0.119	0.060	0.040
-4.155	-0.103	0.090	0.060
-3.668	-0.087	0.116	0.073
-3.178	-0.070	0.175	0.101
-2.695	-0.055	0.243	0.121
-2.230	-0.039	0.303	0.141
-1.717	-0.023	0.382	0.152
-1.191	-0.005	0.465	0.158
-0.683	0.011	0.546	0.158
-0.183	0.028	0.644	0.155
0.386	0.046	0.750	0.147
0.818	0.061	0.831	0.139
1.308	0.077	0.898	0.115
1.796	0.093	0.952	0.083
2.256	0.108	0.983	0.059
2.807	0.126	0.997	0.038
3.698	0.155	1.000	0.026
5.243	0.206	1.000	0.012

z=m*y+b; 1/m=2.170 cm; y(.5)=-b/m=-1.030 cm

L.B.L. 1/8/77 x=38.10 cm Umax=18.66 mps

y(cm)	$\frac{y-y(.5)}{x}$	$\frac{U}{Umax}$	$\frac{U'}{Umax}$
-9.604	-0.222	0.031	0.012
-8.783	-0.201	0.030	0.013
-6.670	-0.145	0.044	0.023
-5.682	-0.119	0.061	0.039
-5.182	-0.106	0.081	0.051
-4.704	-0.094	0.103	0.063
-4.229	-0.081	0.134	0.083
-3.698	-0.067	0.178	0.102
-3.178	-0.054	0.235	0.119
-2.687	-0.041	0.290	0.134
-2.197	-0.028	0.337	0.146
-1.712	-0.015	0.416	0.156
-1.191	-0.001	0.490	0.161
-0.676	0.012	0.565	0.164
-0.190	0.025	0.642	0.164
0.251	0.036	0.721	0.155
0.792	0.051	0.795	0.145
1.275	0.063	0.867	0.129
1.740	0.076	0.912	0.113
2.296	0.090	0.965	0.082
2.771	0.103	0.985	0.061
3.251	0.115	0.995	0.043
3.754	0.128	0.998	0.034
4.244	0.141	1.000	0.029
6.228	0.193	0.999	0.015

z=m*y+b; 1/m=2.429 cm; y(.5)=-b/m=-1.137 cm

L.B.L. 1/8/77 x=50.80 cm Umax=18.66 mps

y(cm)	$\frac{y-y(.5)}{x}$	$\frac{U}{Umax}$	$\frac{U'}{Umax}$
-9.629	-0.160	0.033	0.018
-9.147	-0.150	0.038	0.020
-8.618	-0.140	0.044	0.025
-7.643	-0.121	0.057	0.034
-7.173	-0.111	0.067	0.043
-6.673	-0.101	0.080	0.052
-6.251	-0.093	0.102	0.067
-5.639	-0.081	0.135	0.085
-5.166	-0.072	0.160	0.093
-4.671	-0.062	0.200	0.110
-4.183	-0.052	0.218	0.114
-3.673	-0.042	0.266	0.131
-3.167	-0.032	0.308	0.140
-2.695	-0.023	0.377	0.149
-2.212	-0.014	0.413	0.150
-1.697	-0.004	0.474	0.161
-1.217	0.006	0.523	0.165
-0.607	0.018	0.617	0.163
-0.109	0.028	0.661	0.162
0.404	0.038	0.726	0.153
0.767	0.045	0.776	0.148
1.341	0.056	0.832	0.137
1.841	0.066	0.882	0.121
2.281	0.075	0.922	0.106
2.776	0.085	0.957	0.083
3.167	0.092	0.972	0.071
3.599	0.101	0.984	0.059
4.054	0.110	0.992	0.050
4.442	0.117	0.996	0.044
4.956	0.127	0.998	0.037
5.537	0.139	1.000	0.030
6.228	0.152	0.999	0.028

z=m*y+b; 1/m=3.305 cm; y(.5)=-b/m=-1.518 cm

T.B.L. 1/22/77 x= 2.54 cm Umax=18.25 mps

y(cm)	y-y(.5)/x	U/Umax	U'/Umax
-0.538	-0.211	0.035	0.017
-0.411	-0.161	0.064	0.037
-0.323	-0.126	0.103	0.059
-0.264	-0.103	0.161	0.081
-0.224	-0.087	0.205	0.093
-0.178	-0.069	0.253	0.104
-0.142	-0.055	0.299	0.112
-0.066	-0.025	0.396	0.122
0.076	0.031	0.613	0.123
0.076	0.031	0.618	0.123
0.142	0.057	0.709	0.115
0.188	0.075	0.764	0.104
0.269	0.107	0.842	0.079
0.363	0.144	0.897	0.061
0.518	0.205	0.953	0.046
0.744	0.294	0.993	0.021
1.026	0.405	1.000	0.004

z=m*y+b; 1/m=0.257 cm; y(.5)=-b/m=-0.002 cm

T.B.L. 1/22/77 x= 5.08 cm Umax=18.10 mps

y(cm)	y-y(.5)/x	U/Umax	U'/Umax
-0.808	-0.151	0.039	0.021
-0.635	-0.117	0.078	0.047
-0.556	-0.101	0.105	0.061
-0.472	-0.085	0.150	0.079
-0.396	-0.070	0.195	0.093
-0.302	-0.051	0.269	0.109
-0.236	-0.038	0.320	0.117
-0.130	-0.017	0.415	0.127
-0.030	0.002	0.506	0.129
0.084	0.025	0.620	0.128
0.180	0.044	0.699	0.123
0.241	0.056	0.768	0.114
0.295	0.066	0.814	0.102
0.338	0.075	0.847	0.092
0.442	0.095	0.913	0.071
0.536	0.114	0.951	0.044
0.935	0.192	1.000	0.010

z=m*y+b; 1/m=0.411 cm; y(.5)=-b/m=-0.041 cm

T.B.L. 1/22/77 x= 7.62 cm Umax=18.23 mps

y(cm)	y-y(.5)/x	U/Umax	U'/Umax
-1.285	-0.158	0.031	0.015
-1.034	-0.125	0.049	0.029
-0.881	-0.105	0.074	0.046
-0.762	-0.090	0.107	0.063
-0.721	-0.084	0.120	0.069
-0.676	-0.078	0.139	0.077
-0.638	-0.073	0.160	0.084
-0.559	-0.063	0.192	0.093
-0.429	-0.046	0.260	0.110
-0.295	-0.028	0.343	0.123
-0.213	-0.018	0.395	0.129
-0.117	-0.005	0.471	0.133
-0.053	0.003	0.517	0.135
0.076	0.020	0.612	0.132
0.208	0.038	0.716	0.126
0.345	0.056	0.816	0.113
0.437	0.068	0.873	0.096
0.513	0.078	0.915	0.079
0.610	0.090	0.954	0.057
0.757	0.110	0.987	0.033
1.133	0.159	1.000	0.012
1.816	0.249	0.999	0.004

z=m*y+b; 1/m=0.503 cm; y(.5)=-b/m=-0.078 cm

T.B.L. 1/22/77 x=10.16 cm Umax=18.23 mps

y(cm)	y-y(.5)/x	U/Umax	U'/Umax
-1.689	-0.154	0.031	0.016
-1.300	-0.116	0.050	0.030
-1.300	-0.116	0.051	0.031
-0.952	-0.082	0.114	0.067
-0.815	-0.068	0.153	0.083
-0.719	-0.059	0.192	0.096
-0.513	-0.038	0.280	0.117
-0.381	-0.025	0.346	0.128
-0.257	-0.013	0.413	0.135
-0.145	-0.002	0.482	0.140
0.030	0.015	0.592	0.139
0.119	0.024	0.650	0.138
0.236	0.035	0.726	0.133
0.323	0.044	0.776	0.126
0.452	0.057	0.847	0.114
0.549	0.066	0.904	0.095
0.676	0.079	0.950	0.072
0.831	0.094	0.986	0.044
1.113	0.122	0.999	0.025
1.448	0.155	0.999	0.014
1.816	0.191	1.000	0.007

z=m*y+b; 1/m=0.605 cm; y(.5)=-b/m=-0.123 cm

T.B.L. 1/22/77 x=15.24 cm Umax=18.07 mps

y(cm)	$\frac{y-y(.5)}{x}$	$\frac{U}{Umax}$	$\frac{U'}{Umax}$
-2.090	-0.119	0.046	0.026
-1.875	-0.105	0.060	0.036
-1.633	-0.089	0.084	0.052
-1.392	-0.074	0.122	0.072
-1.262	-0.065	0.151	0.085
-1.113	-0.055	0.187	0.098
-0.993	-0.047	0.217	0.107
-0.876	-0.040	0.257	0.118
-0.742	-0.031	0.303	0.128
-0.615	-0.023	0.348	0.134
-0.432	-0.011	0.424	0.144
-0.259	0.001	0.499	0.149
0.000	0.018	0.619	0.149
0.196	0.031	0.708	0.145
0.262	0.035	0.745	0.142
0.457	0.048	0.835	0.130
0.566	0.055	0.870	0.118
0.747	0.067	0.936	0.094
1.163	0.094	1.000	0.035

z=m*y+b; 1/m=0.821 cm; y(.5)=-b/m=-0.269 cm

T.B.L. 1/22/77 x=20.32 cm Umax=18.16 mps

y(cm)	$\frac{y-y(.5)}{x}$	$\frac{U}{Umax}$	$\frac{U'}{Umax}$
-3.538	-0.153	0.041	0.021
-2.814	-0.118	0.056	0.031
-2.304	-0.093	0.082	0.049
-1.900	-0.073	0.127	0.073
-1.709	-0.063	0.152	0.085
-1.516	-0.054	0.188	0.100
-1.265	-0.041	0.243	0.117
-1.074	-0.032	0.289	0.128
-0.696	-0.013	0.400	0.147
-0.439	-0.001	0.490	0.155
-0.130	0.014	0.599	0.157
0.135	0.027	0.692	0.152
0.277	0.034	0.739	0.148
0.444	0.043	0.794	0.142
0.571	0.049	0.838	0.134
0.632	0.052	0.859	0.130
0.848	0.063	0.913	0.110
1.245	0.082	0.979	0.069
1.720	0.105	1.000	0.043
1.758	0.107	1.000	0.041

z=m*y+b; 1/m=1.100 cm; y(.5)=-b/m=-0.424 cm

T.B.L. 1/22/77 x=25.40 cm Umax=18.20 mps

y(cm)	$\frac{y-y(.5)}{x}$	$\frac{U}{Umax}$	$\frac{U'}{Umax}$
-4.046	-0.134	0.053	0.027
-3.561	-0.115	0.067	0.037
-2.931	-0.091	0.095	0.055
-2.532	-0.075	0.130	0.075
-2.393	-0.069	0.144	0.081
-2.085	-0.057	0.185	0.099
-1.687	-0.042	0.251	0.120
-1.440	-0.032	0.296	0.133
-0.975	-0.014	0.400	0.150
-0.635	0.000	0.493	0.157
-0.272	0.014	0.593	0.159
0.183	0.032	0.714	0.154
0.361	0.039	0.766	0.148
0.752	0.054	0.861	0.129
1.011	0.065	0.910	0.115
1.313	0.077	0.952	0.092
1.788	0.095	0.989	0.062
2.809	0.135	1.000	0.035

z=m*y+b; 1/m=1.398 cm; y(.5)=-b/m=-0.632 cm

T.B.L. 1/22/77 x=30.48 cm Umax=18.15 mps

y(cm)	$\frac{y-y(.5)}{x}$	$\frac{U}{Umax}$	$\frac{U'}{Umax}$
-5.489	-0.153	0.050	0.025
-4.663	-0.126	0.059	0.031
-3.932	-0.102	0.083	0.047
-3.449	-0.086	0.108	0.062
-2.850	-0.067	0.154	0.087
-2.230	-0.046	0.228	0.117
-1.661	-0.028	0.322	0.141
-1.204	-0.013	0.413	0.155
-0.818	0.000	0.491	0.161
-0.343	0.015	0.598	0.165
0.109	0.030	0.701	0.157
0.450	0.041	0.775	0.144
0.450	0.041	0.777	0.148
0.930	0.057	0.867	0.130
1.283	0.069	0.917	0.114
1.605	0.079	0.954	0.094
2.090	0.095	0.988	0.070
2.479	0.108	0.998	0.055
2.809	0.119	1.000	0.048

z=m*y+b; 1/m=1.698 cm; y(.5)=-b/m=-0.813 cm

T.B.L. 1/22/77 x=35.56 cm Umax=18.22 mps

y(cm)	$\frac{y-y(.5)}{x}$	$\frac{U}{Umax}$	$\frac{U'}{Umax}$
-5.489	-0.125	0.060	0.032
-5.194	-0.117	0.068	0.038
-4.491	-0.097	0.093	0.055
-4.260	-0.091	0.102	0.060
-3.813	-0.078	0.131	0.076
-3.513	-0.070	0.152	0.086
-2.979	-0.055	0.200	0.108
-2.497	-0.041	0.254	0.126
-2.126	-0.031	0.306	0.140
-1.565	-0.015	0.394	0.156
-0.973	0.002	0.503	0.164
-0.404	0.018	0.610	0.164
0.175	0.034	0.720	0.154
0.417	0.041	0.765	0.149
0.622	0.046	0.797	0.146
1.046	0.058	0.860	0.131
1.346	0.067	0.900	0.120
1.913	0.083	0.954	0.094
2.758	0.107	0.992	0.060
3.818	0.136	1.000	0.037

z=m*y+b; 1/m=2.105 cm; y(.5)=-b/m=-1.031 cm

T.B.L. 1/22/77 x=40.64 cm Umax=18.17 mps

y(cm)	$\frac{y-y(.5)}{x}$	$\frac{U}{Umax}$	$\frac{U'}{Umax}$
-6.838	-0.138	0.051	0.027
-5.583	-0.107	0.076	0.045
-4.762	-0.087	0.111	0.067
-4.013	-0.068	0.163	0.093
-3.459	-0.055	0.206	0.112
-3.018	-0.044	0.251	0.126
-2.497	-0.031	0.307	0.142
-1.709	-0.012	0.420	0.161
-1.140	0.002	0.505	0.168
-0.541	0.017	0.602	0.170
0.056	0.032	0.701	0.160
0.462	0.042	0.763	0.153
0.762	0.049	0.808	0.146
0.762	0.049	0.808	0.146
1.090	0.057	0.850	0.137
1.600	0.070	0.908	0.118
2.286	0.087	0.961	0.090
2.954	0.103	0.985	0.068
3.299	0.112	0.994	0.057
4.135	0.132	1.000	0.043

z=m*y+b; 1/m=2.508 cm; y(.5)=-b/m=-1.232 cm

T.B.L. 1/22/77 x=50.80 cm Umax=18.08 mps

y(cm)	$\frac{y-y(.5)}{x}$	$\frac{U}{Umax}$	$\frac{U'}{Umax}$
-7.889	-0.123	0.060	0.037
-7.087	-0.107	0.081	0.052
-6.256	-0.091	0.108	0.070
-5.555	-0.077	0.140	0.087
-4.821	-0.063	0.184	0.107
-3.924	-0.045	0.262	0.133
-3.358	-0.034	0.306	0.146
-2.362	-0.014	0.412	0.166
-1.773	-0.003	0.478	0.171
-1.438	0.004	0.515	0.173
-0.622	0.020	0.620	0.174
0.097	0.034	0.705	0.163
0.531	0.043	0.765	0.156
1.054	0.053	0.821	0.143
1.422	0.060	0.861	0.134
2.024	0.072	0.907	0.116
2.939	0.090	0.963	0.087
3.876	0.108	0.991	0.065
5.093	0.132	1.000	0.036

z=m*y+b; 1/m=3.222 cm; y(.5)=-b/m=-1.629 cm